

AFTT/GA/ENY/93D-9

AD-A273 732



2

DTIC
ELECTE
DEC 16 1993
S A

**THE MODAL SOLUTION TO THE
MOON'S ORBIT USING CANONICAL
FLOQUET PERTURBATION THEORY**

THESIS

Kurt A. Vogel, Captain, USAF

AFTT/GA/ENY/93D-9

Approved for public release; Distribution Unlimited

93-30470



93 12 15 08 6

THE MODAL SOLUTION TO THE MOON'S ORBIT USING
CANONICAL FLOQUET PERTURBATION THEORY

THESIS

Presented to the Faculty of the Graduate School of Engineering

of the Air Force Institute of Technology

Air University

In Partial Fulfillment of the

Requirements for the Degree of

Master of Science in Astronautical Engineering

Kurt A. Vogel, B.S.

Captain, USAF

December 1993

Accession For		
NTIS	CRA&I	<input checked="" type="checkbox"/>
DTIC	TAB	<input type="checkbox"/>
Unannounced		<input type="checkbox"/>
Justification		
By		
Distribution /		
Availability Codes		
Dist	Avail and/or Special	
A-1		



Approved for public release; Distribution Unlimited

Acknowledgments

I would first like to thank Dr William E. Wiesel, my advisor, without whom this work would not have been possible. Dr Wiesel built the foundation for this study in many ways. Besides introducing the original idea for this thesis, he provided personal direction and contributions that were invaluable to my understanding of the concepts.

To my parents, Claude and Judy Vogel, I want to express how grateful I am for all the love and encouragement they have shown me over the years. I owe every success that I now enjoy to their continuing optimism and reassurances that *things will always work out in the end*. I feel incredibly lucky to have been blessed with my parents. They have always urged me to do what makes me the happiest, and thanks to them it appears that I have got quite a blissful future to look forward to.

Most importantly, I would like to thank my beautiful wife, Tracy. For sacrificing some of the things that were important to her for the last eighteen months; for volunteering to take the extra responsibilities off of my shoulders; for comforting and supporting me when things got frustrating; for waiting up most nights and sleeping alone others, all without protest. I dedicate this thesis with all of my love to you, Tracy.

- Kurt A. Vogel

Table of Contents

	page
Acknowledgments.....	ii
List of Figures.....	v
List of Symbols.....	vii
Abstract.....	x
 I. Introduction.....	 1
 II. Historical Development.....	 3
2.1 Dynamics.....	3
2.2 Floquet Reference Solutions.....	3
2.3 Canonical Floquet Theory.....	3
2.4 Application.....	4
 III. Theory.....	 5
3.1 Dynamics.....	5
3.2 Periodic Orbits.....	11
3.3 Classical Floquet Theory.....	18
3.4 Canonical Floquet Theory.....	21
3.5 Symplectic Normalization.....	23
3.6 Modal Variable Development.....	25
3.7 Actual Lunar Orbit.....	37
3.8 Perturbation Theory.....	51
 IV. Software.....	 54
4.1 Periodic Orbit.....	54
4.2 Symplectic Normalization.....	54
4.3 Modal Variable Development.....	55
4.4 Real Moon Initial Conditions from Data (Exact Solution).....	55
4.5 Expanded Modal Solution.....	56
 V. Results and Discussion.....	 57
5.1 Exact Modal Results.....	57
5.2 Expanded Modal Results.....	61
5.3 Complex Conjugacy.....	76
 VI. Conclusions and Recommendations.....	 77

Appendix A: Monodromy Matrix, Initial Eigenvector Matrix, and J Matrix	79
Appendix B: Ephemerides from February 1967.....	83
Appendix C: Ephemerides from February 1986.....	84
Bibliography.....	85
Vita.....	87

List of Figures

	page
1. The Restricted Three Body Coordinate System.	7
2. Periodic Orbit in the Restricted Three Body Problem.	15
3. Two Body Initial Guess in the Restricted Three Body Coordinates.	17
4. Time/Energy Mode using Periodic Orbit Initial Conditions.	28
5. Inclination Mode using Periodic Orbit Initial Conditions.	29
6. Eccentricity Mode using Periodic Orbit Initial Conditions.	30
7. Time/Energy Mode using Initial Conditions in the Linear Region.	31
8. Inclination Mode using Initial Conditions in the Linear Region.	32
9. Eccentricity Mode using Initial Conditions in the Linear Region.	33
10. Time/Energy Mode using Initial Conditions Beyond the Linear Region.	34
11. Inclination Mode using Initial Conditions Beyond the Linear Region.	35
12. Eccentricity Mode using Initial Conditions Beyond the Linear Region.	36
13. Horizontal Parallax.	38
14. Data Gathered from Ephemerides.	38
15. Earth Centered Rotating (ECR) Coordinate Frame.	39
16. Polar Coordinates Relative to the ECR Frame.	40
17. Rectangular ECR Coordinates from the Polar Coordinates.	40
18. Time/Energy Mode using Preliminary Lunar Orbit Initial Conditions.	44
19. Inclination Mode using Preliminary Lunar Orbit Initial Conditions.	45
20. Eccentricity Mode using Preliminary Lunar Orbit Initial Conditions.	46
21. Periodic Orbit and Preliminary Lunar Orbit in Physical Space. X and Y components of the Restricted Three Body Problem.	48

22. Exact Modal Representation of the Time/Energy Mode using Fitted Initial Conditions.	58
23. Exact Modal Representation of the Inclination Mode using Fitted Initial Conditions.	59
24. Exact Modal Representation of the Eccentricity Mode using Fitted Initial Conditions.	60
25. Exact vs Expanded Modal Solution (K2 Only). Time/Energy Mode.	63
26. Exact vs Expanded Modal Solution (K2 Only). Inclination Mode.	64
27. Exact vs Expanded Modal Solution (K2 Only). Eccentricity Mode.	65
28. Exact vs Expanded Modal Solution (K2 & K3 Only). Time/Energy Mode.	66
29. Exact vs Expanded Modal Solution (K2 & K3 Only). Inclination Mode.	67
30. Exact vs Expanded Modal Solution (K2 & K3 Only). Eccentricity Mode.	68
31. Exact vs Expanded Modal Solution (K2, K3 & K4). Time/Energy Mode.	69
32. Exact vs Expanded Modal Solution (K2, K3 & K4). Inclination Mode.	70
33. Exact vs Expanded Modal Solution (K2, K3 & K4). Eccentricity Mode.	71
34. Exact vs Expanded Modal Solution (K2, K3 & K4) for Fictitious Moon. Time/Energy Mode.	73
35. Exact vs Expanded Modal Solution (K2, K3 & K4) for Fictitious Moon. Inclination Mode.	74
36. Exact vs Expanded Modal Solution (K2, K3 & K4) for Fictitious Moon. Eccentricity Mode.	75

List of Symbols

A	System Linearization Matrix
a	Scaling Interpolation Variable
$\hat{\mathbf{b}}$	Earth Centered Rotating Coordinate Frame
D	Diagonal, Symplectic Normalization Matrix
E	Symplectically Normalized System Eigenvector Matrix
$\bar{\epsilon}$	Error in Physical State Variables
F	System Eigenvector Matrix
\bar{f}_i	Eigenvector
\bar{f}_i'	Generalized Eigenvector
G	Universal Gravitational Constant
h	Step Size in an Interpolation
\mathcal{H}	Hamiltonian in Physical Variables
I	Identity Matrix
J	Jordan Normal Matrix of System Frequencies (Poincaré Exponents)
\mathcal{K}	Hamiltonian in Modal Variables
\mathcal{L}	Lagrangian
lat_m	Apparent Latitude of the Moon wrt the Ecliptic Plane
lon_m	Apparent Longitude of the Moon from the Vernal Equinox in the Ecliptic Plane
δlon_m	Longitude of the Moon in the Earth Centered Rotating Frame
lon_s	Longitude of the Sun from the Vernal Equinox in the Ecliptic Plane
M_1	Mass of the Sun

M_2	Mass of the Earth
M_3	Mass of the Moon
m_1	Dimensionless Mass of the Sun
m_2	Dimensionless Mass of the Earth
m_3	Dimensionless Mass of the Moon
n	Mean Motion of the Restricted Three Body Coordinate Frame
\bar{p}	Generalized Momentum Vector
p_i	Generalized Momenta
\bar{q}	Generalized Coordinate Vector
q_i	Generalized Coordinates
R	Distance between the Earth and Moon
R_{moon}	Average Distance between the Earth and Moon
R_\oplus	Radius of the Earth
\bar{r}	Moon's Position in the Restricted Three Body Coordinates (also \bar{q})
\bar{r}_{BCR}	Moon's Position in the Earth Centered Rotating Frame
\bar{r}'	Moon's Velocity wrt the Restricted Three Body Frame
\bar{r}_1	Moon's Position wrt the Sun in Restricted Three Body Coordinates
\bar{r}_2	Moon's Position wrt the Earth in Restricted Three Body Coordinates
S_1	Distance of the Sun from the Center of Mass of the Earth/Sun System
S_2	Distance of the Earth from the Center of Mass of the Earth/Sun System
s_1	Dimensionless Distance of the Sun from the Center of Mass of the Earth/Sun System
s_2	Dimensionless Distance of the Earth from the Center of Mass of the Earth/Sun System

T	Kinetic Energy of the Moon
u_i	Ephemeris Time for Interpolation
V	Potential Energy of the Moon
\bar{v}	Moon's Inertial Velocity in terms of the Restricted Three Body Coordinates
\bar{x}	Moon's State Vector in Physical Variables
\bar{x}_p	Periodic Orbit's State Vector in Physical Variables
$\delta\bar{x}$	Variation of the Moon's State in Physical Variables
\bar{y}	Modal State Vector
y_i	Modal Variable
Z	Correlation Matrix
λ_i	System Eigenvalues
μ	Dimensionless Mass/Distance Parameter
Π_m	Horizontal Parallax of the Moon
τ	Period of the Moon in Restricted Three Body Coordinates
τ_\oplus	Orbital Period of the Earth Around the Sun
$\Phi(t, t_0)$	State Transition Matrix
$\Phi(\tau, 0)$	Monodromy Matrix
ω	Angular Velocity of the Restricted Three Body Coordinate Frame
ω_i	System Frequencies (Poincaré Exponents)

Abstract

Using the restricted three body problem, the equations of motion (EOM) and Hamiltonian are computed for the moon's orbit in physical variables. A periodic orbit is found in the vicinity of the moon's orbit, and classical Floquet theory is applied to the periodic orbit to give stability information and the complete solution to the equations of variation. Floquet theory also supplies a transformation from physical variables to modal variables. This transformation to modal variables is made canonical by constraining the initial transformation matrix to be symplectic. Actual lunar data is used to calculate the modes for the real moon's orbit. Once satisfied that the moon's real-world modes are in (or near) the linear regime of the periodic orbit, the modal EOM are found by doing a perturbation expansion on the new modal Hamiltonian. The modal results from the real lunar orbit are compared with the modal EOM/expansion results. The modal expansion proves to be an accurate solution to the moon's orbit given enough expansion terms.

THE MODAL SOLUTION TO THE MOON'S ORBIT USING CANONICAL FLOQUET PERTURBATION THEORY

I. Introduction

The study of the Lunar Theory, which is essentially a particular case of the three body problem, began in 1687 with the introduction of Sir Isaac Newton's *Principia*. Significant contributions were made over the last three centuries including those by D' Alembert, Euler, and Laplace, however most of these approaches are implicitly based on two body, Keplerian orbits as reference trajectories for classical analytic perturbation techniques. The first real departure from this classical Lunar Theory wasn't until 1877 when G.W. Hill expanded on Euler's three body problem by choosing rectangular coordinates that rotate with the Sun's mean angular velocity instead of the moon's mean angular velocity. In addition, Hill made some simplifications to what is now known as the restricted three body problem. The result of Hill's work is a periodic reference orbit in the three body problem coordinates.

One hundred years later, in 1981, Wiesel demonstrated the concept of applying the classical Floquet problem to the periodic reference orbit to get a Floquet mode reference solution. The advantage of this over the classical reference solutions is that the Floquet modes already include some perturbing characteristics (such as precession of the orbit plane) *in* the reference solution, before the perturbation analysis is done. More recently, Wiesel and Pohlen (1992) improved on the concept by constraining the Floquet transformation to modal variables to be canonical. The result is a canonical Floquet reference solution that is quite applicable for the Lunar Theory. However, while Pohlen (1992) did illustrate its utility with a Sun-Jupiter restricted three body example, this reference solution technique has not yet been validated with real celestial data or for a three dimensional case.

The purpose of this study is to construct the three dimensional application of the restricted three body canonical Floquet reference solution to a celestial body for which we have a plethora of historical data: the moon. Specifically, we will find a periodic orbit in the vicinity of the moon (Hill's orbit), get the Floquet modes, canonicalize them, constrain the dynamics to match the real data, and finally get the modal reference solution. This work accomplishes three things:

1. It provides a second, dynamically more challenging system to demonstrate canonical Floquet theory.
2. It investigates the applicability of the canonical Floquet theory to an actual system that is constrained to obey historical data.
3. It lays the foundation for applying further analytic perturbation techniques to the moon's modal solution as a reference trajectory.

Chapter Two identifies the specific background work that was done prior to this study, and explains the differences between this and previous applications of Floquet reference solutions. Chapter Three is a detailed discussion of the theory used to investigate the modal solution, while the actual software used to implement the theory is described in Chapter Four. Chapter Five is the results. It includes an analysis of the modal solution as well as real moon's linearity with respect to the periodic orbit.

II. Historical Development

2.1 Dynamics

The groundwork for the restricted three body problem was laid out by Euler in 1772. In applying this restricted three body problem to the Lunar Theory, Hill made some simplifications that give us the foundation for our dynamic model. Plenty of information was available on this subject (Brouwer and Clemence, 1961:336 or Szebehely, 1967:602).

2.2 Floquet Reference Solutions

Since 1883, classical Floquet analysis of periodic systems was a common technique only in so far as determining stability information. The idea of expanding the utility of Floquet theory to get perturbation reference solutions for periodic orbits was introduced by Dr. Wiesel in 1980. As mentioned in Chapter One, Dr. Wiesel then went on to develop Floquet mode reference solutions specifically for the Lunar Theory in 1981. This Floquet perturbation theory for periodic orbits was further demonstrated by Ross (1991). His work was actually the first to apply the classical Floquet perturbation theory to a system using the restricted three body problem for the dynamics. The system Ross chose was the Sun-Jupiter system.

2.3 Canonical Floquet Theory

The classical Floquet problem naturally introduced a transformation from physical variables to modal variables. The next step in the development of this theory was made by Wiesel and Pohlen (1992) in realizing that this Floquet transformation needed to be canonical. In their paper, they presented the method for making the transformation canonical which enabled canonical perturbation theory to be applied properly to Hamiltonian systems. Finally, Pohlen (1992) illustrated this canonical Floquet perturbation theory by applying it to the same

restricted three body problem done by Ross (1991). Like Ross, Pohlen used the Sun-Jupiter system because its high mass ratio made it a good diagnostic case.

2.4 Application

The restricted three body system used by Ross and Pohlen was confined to two dimensions. Because of the moon's out-of-plane motion, the problem in this work is expanded to three dimensions. Also, in Pohlen's study, an effort was made to transform complex eigensystems into real eigensystems to yield real modal vectors. In this study, we allow the eigensystems and resulting modal vectors to be complex. Finally, where Pohlen used the restricted three body Sun-Jupiter model as the exact representation of the modal solution, we go on to constrain the Sun-Earth-Moon model to obey actual moon ephemerides.

III. Theory

3.1 Dynamics

The first step to finding the complete modal solution is to decide on the dynamic model to be used for the system. In this case, the system consists of the earth and moon, the sun, and other lower order perturbing contributors. The restricted three-body problem (R3B) is used to define the dynamics of the earth-sun-moon system. Perturbation theory will account for the omitted terms.

3.1.1 The Restricted Three-Body Problem

The general restricted three-body problem was first introduced by Leonard Euler in his memoir on his second lunar theory in 1772. The definition, according to Szebehely, is this:

Two point masses m_1 and m_2 called the primaries revolve around their center of mass in circular orbits. In the plane of their motion moves a third body with infinitesimal mass, not influencing the motion of the primaries. Assuming Newtonian gravitational forces, find the behavior of the third body. (Szebehely, 1967:557)

In this study, we assume the conditions above are applicable where the two primaries are the earth and sun, and the body of interest (the third body) is the moon. We assume that the earth and sun are both point masses and significantly more massive than the moon, and that the moon has a negligible affect on the earth and sun. What we now have is the basic setup for G. W. Hill's approach to lunar theory. Hill took the general restricted three-body problem, applied the earth-sun-moon system, and made three simplifications to the system:

1. The solar parallax is zero. The disturbing function is truncated.
2. The lunar inclination is zero.
3. The solar eccentricity is zero.

Further details of Hill's method can be found in either Brouwer and Clemence (1961:336) or Szebehely (1967:602).

Before the coordinate system for this problem is established, we need to introduce some dimensionless variables for mass, length and time:

$$\begin{aligned} m_1 &= \frac{M_1}{M_1 + M_2} & m_2 &= \frac{M_2}{M_1 + M_2} & m_3 &= \frac{M_3}{M_1 + M_2} \approx 0 \\ s_1 &= \frac{S_1}{S_1 + S_2} & s_2 &= \frac{S_2}{S_1 + S_2} \end{aligned} \quad (1)$$

where M_1 , M_2 , and M_3 are the masses of the sun, earth, and moon respectively. S_1 and S_2 are the distances of the sun and earth from the center of mass of the system. The total dimensionless distance between the earth and sun is set equal to one, as is the total dimensionless mass of the two primaries.

$$s_1 + s_2 = 1 \quad m_1 + m_2 = 1 \quad (2)$$

Using the definition for center of mass position (s_1) with respect to m_1 ,

$$s_1 = \frac{\sum m_i s_i}{\sum m_i} = \frac{m_1 \cdot 0 + m_2 (s_1 + s_2)}{m_1 + m_2} = m_2 \quad (3)$$

we can now define all four dimensionless variables in terms of one non-dimensional parameter, μ :

$$\begin{aligned} s_1 &= m_2 \equiv \mu \\ s_2 &= m_1 = 1 - \mu \end{aligned} \quad (4)$$

The orbital period, τ_\oplus , of the earth around the sun is also defined using the dimensionless parameters as

$$\tau_\oplus = 2\pi \sqrt{\frac{(s_1 + s_2)^3}{G(m_1 + m_2)}} \quad (5)$$

where G is the universal gravitational constant. If G is set to one, $\tau_\oplus = 2\pi$. In addition, the angular velocity, ω , of the primaries about the center of mass is

$$\omega = n = \sqrt{\frac{G(m_1 + m_2)}{(s_1 + s_2)^3}} = 1 \quad (6)$$

A synodic coordinate system is used as defined by Szebehely (1967:9) where the origin is the center of mass of the two primaries. The X-axis is a line between the sun and earth. The sun is a distance μ from the origin in the positive X direction, while the earth is $(1-\mu)$ in the negative X direction. The Y-axis is such that the XY plane defines the plane in which the primaries rotate. The coordinate system is synodic since the X and Y axes rotate *with* the primaries around the center of mass/origin (see Figure 1). The vectors \bar{r} , \bar{r}_1 , and \bar{r}_2 are the position vectors of the moon with respect to the center of mass, the sun, and the earth respectively.

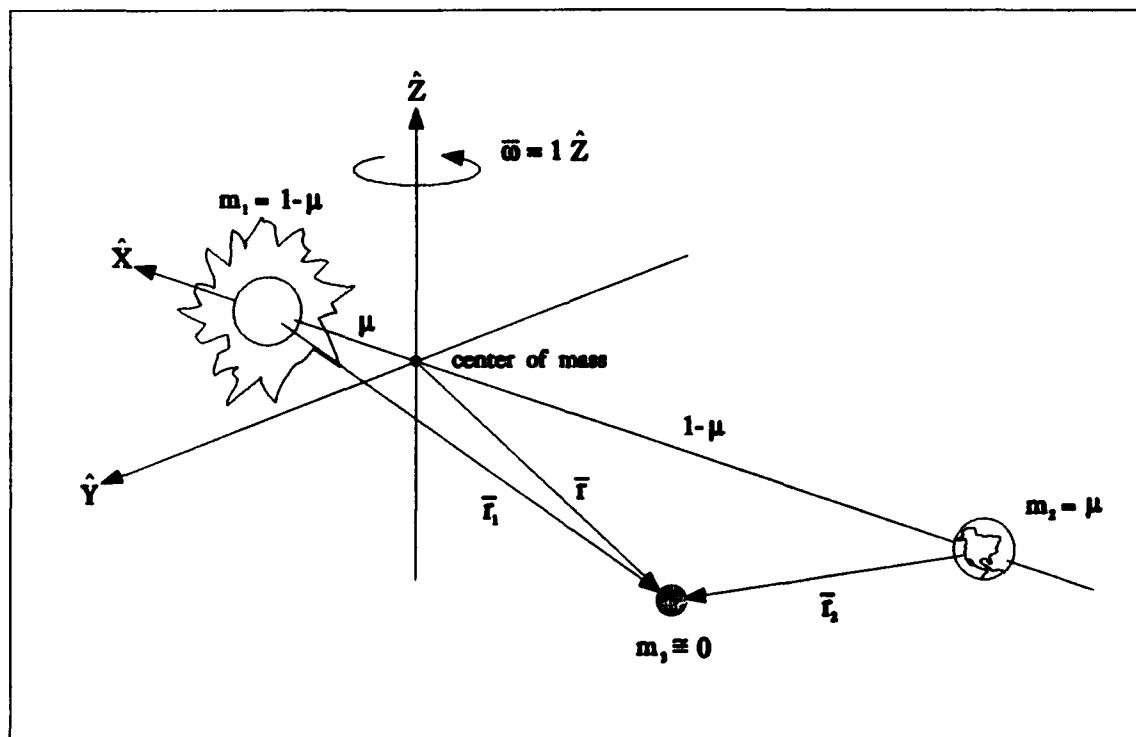


Figure 1. The Restricted Three Body Coordinate System.

This coordinate system is the same as described by Ross, with the addition of the Z-axis. The addition of a third dimension has also been discussed in Szebechely (1967:557).

3.1.2 The Restricted Three-Body Equations of Motion

Let the generalized coordinates (q_i) and momenta (p_i) be defined as

$$q_i = x, y, z \quad p_i = p_x, p_y, p_z$$

Then, the position of the moon with respect to the center of mass is

$$\bar{\mathbf{r}} = \begin{pmatrix} x \\ y \\ z \end{pmatrix} \quad \text{or} \quad \bar{\mathbf{r}} = x\hat{\mathbf{X}} + y\hat{\mathbf{Y}} + z\hat{\mathbf{Z}} \quad (7)$$

and the inertial velocity of the moon in terms of X, Y, Z coordinates is

$$\begin{aligned} \bar{\mathbf{v}} &= \dot{\bar{\mathbf{r}}} + (\bar{\boldsymbol{\omega}} \times \bar{\mathbf{r}}) = \begin{pmatrix} \dot{x} \\ \dot{y} \\ \dot{z} \end{pmatrix} + \begin{pmatrix} -y \\ x \\ 0 \end{pmatrix} \\ &= \begin{pmatrix} \dot{x} - y \\ \dot{y} + x \\ \dot{z} \end{pmatrix} \end{aligned} \quad (8)$$

Using Eqs (7) and (8), the kinetic (T) and potential (V) energies of the moon are calculated as well as the specific Lagrangian (\mathcal{L}):

$$T = \frac{1}{2} m_3 \bar{\mathbf{v}} \cdot \bar{\mathbf{v}} = \frac{1}{2} m_3 [(\dot{x} - y)^2 + (\dot{y} + x)^2 + \dot{z}^2] \quad (9)$$

$$\begin{aligned} V &= \frac{-Gm_1m_3}{|\bar{\mathbf{r}}_1|} + \frac{-Gm_2m_3}{|\bar{\mathbf{r}}_2|} \\ &= \frac{-m_3(1-\mu)}{r_1} + \frac{-m_3(\mu)}{r_2} \end{aligned} \quad (10)$$

$$\begin{aligned}\mathcal{L}' &= T - V = m_3 \left\{ \frac{1}{2} [(\dot{x} - y)^2 + (\dot{y} + x)^2 + \dot{z}^2] + \frac{(1 - \mu)}{r_1} + \frac{\mu}{r_2} \right\} \\ \mathcal{L} &= \frac{\mathcal{L}'}{m_3} = \frac{1}{2} [(\dot{x} - y)^2 + (\dot{y} + x)^2 + \dot{z}^2] + \frac{(1 - \mu)}{r_1} + \frac{\mu}{r_2}\end{aligned}\quad (11)$$

where

$$\begin{aligned}r_1 &= |\bar{r}_1| = \sqrt{(x - \mu)^2 + y^2 + z^2} \\ r_2 &= |\bar{r}_2| = \sqrt{(x + 1 - \mu)^2 + y^2 + z^2}\end{aligned}\quad (12)$$

Taking appropriate partial differentials of the Lagrangian gives expressions for the generalized momenta in terms of their conjugate generalized velocities and vice versa:

$$p_x = \frac{\partial \mathcal{L}}{\partial \dot{x}} = \dot{x} - y \qquad \dot{x} = p_x + y \quad (13)$$

$$p_y = \frac{\partial \mathcal{L}}{\partial \dot{y}} = \dot{y} + x \qquad \dot{y} = p_y - x \quad (14)$$

$$p_z = \frac{\partial \mathcal{L}}{\partial \dot{z}} = \dot{z} \qquad \dot{z} = p_z \quad (15)$$

The Hamiltonian, \mathcal{H} , is now defined as

$$\mathcal{H} = \sum p_i \dot{q}_i - \mathcal{L} \quad (16)$$

only after eliminating the \dot{q}_i 's in favor of the p_i 's. Substituting Equations (11) and (13-15) into Equation (16) yields

$$\mathcal{H} = \frac{1}{2} (p_x^2 + p_y^2 + p_z^2) + p_x y - p_y x - \frac{(1 - \mu)}{r_1} - \frac{\mu}{r_2} \quad (17)$$

To get the equations of motion for the state vector

$$\bar{x}^T = [x, y, z, p_x, p_y, p_z]$$

we use the *Hamilton canonical equations*:

$$\dot{q}_i = \frac{\partial \mathcal{H}}{\partial p_i}, \quad \dot{p}_i = -\frac{\partial \mathcal{H}}{\partial q_i}, \quad i = 1, 2, 3 \quad (18)$$

Therefore, the equations of motion for this problem are

$$\dot{x} = \frac{\partial \mathcal{H}}{\partial p_x} = p_x + y$$

$$\dot{y} = \frac{\partial \mathcal{H}}{\partial p_y} = p_y - x$$

$$\dot{z} = \frac{\partial \mathcal{H}}{\partial p_z} = p_z$$

$$\dot{p}_x = -\frac{\partial \mathcal{H}}{\partial x} = p_y - \frac{(1-\mu) \cdot (x-\mu)}{r_1^3} - \frac{\mu \cdot (x+1-\mu)}{r_2^3}$$

$$\dot{p}_y = -\frac{\partial \mathcal{H}}{\partial y} = -p_x - \frac{(1-\mu) \cdot y}{r_1^3} - \frac{\mu \cdot y}{r_2^3}$$

$$\dot{p}_z = -\frac{\partial \mathcal{H}}{\partial z} = -\frac{(1-\mu) \cdot z}{r_1^3} - \frac{\mu \cdot z}{r_2^3} \quad (19)$$

where the p_i 's are the inertial velocity components resolved on the rotating frame.

3.2 Periodic Orbits

In the last section we established the equations of motion (EOM) for the restricted three-body problem. Now we need to determine the initial conditions that create a periodic orbit which generally describes the moon's motion. Obviously, the moon is *not* in a periodic orbit for the restricted problem's coordinate system. Because of eccentricity, inclination, the precession of the plane of the orbit, and many other perturbations, the lunar orbit does not come back to meet itself every month ... *but it comes close*. The supposition is that it comes close enough to at least be in (or near) the linear region of a periodic orbit.

A periodic orbit is one which closes on itself after each revolution. In other words, the initial state vector (of a body in a periodic orbit) will be equal to the state vector at any multiple of the period:

$$\bar{x}(0) = \bar{x}(\tau) \quad (20)$$

However, given uncertainties in the dynamical model, it is difficult to determine what initial conditions should be used to create the periodicity. "In practice, once a set of initial conditions has been chosen and the orbit integrated, one will find that the initial and final conditions will not agree." (Ross, 1991:10). It is useful, therefore, to integrate the equations of variation (EOV) along with the EOM, because the equations of variation allow us to handle nearby orbits. It is due to these equations of variation that we can correlate differences in the boundary conditions to corrections in the initial conditions. As will be discussed shortly, this sets up an obvious iteration for converging on the correct initial conditions that satisfy Eq (20) and create the desired periodic orbit.

3.2.1 Equations of Variation

In order to iterate on the proper initial conditions required for a periodic orbit, it is necessary to integrate the equations of variation as well as the equations of motion. The EOM can be written as

$$\dot{\bar{x}} = Z \frac{\partial \mathcal{H}}{\partial \bar{x}} = f(\bar{x}, t) \quad (21)$$

where Z is the correlation matrix which has the form

$$Z = \begin{Bmatrix} 0 & I \\ -I & 0 \end{Bmatrix}; \quad I = \text{identity matrix} \quad (22)$$

This correlation matrix follows the identities: $Z^T = Z^{-1} = -Z$. If we define the state (\bar{x}) as the periodic trajectory (\bar{x}_p) plus a small variation ($\delta\bar{x}$),

$$\bar{x} = \bar{x}_p + \delta\bar{x} \quad (23)$$

substitute into Eq (21) and expand in a Taylor's series about $\delta\bar{x} = 0$ (or $\bar{x} = \bar{x}_p$), we get the *equations of variation* (Wiesel, 1993:114)

$$\begin{aligned} \delta\dot{\bar{x}} &= \left. \frac{\partial f}{\partial \bar{x}} \right|_{\delta\bar{x}=0} \delta\bar{x} \\ &= Z \left. \frac{\partial^2 \mathcal{H}}{\partial \bar{x}^2} \right|_{\delta\bar{x}=0} \delta\bar{x} \\ &= A(t) \delta\bar{x} \end{aligned} \quad (24)$$

where A is a square matrix of partial derivatives of the equations of motion with respect to the state variables, evaluated on the periodic trajectory. It is a function of time only. For this study the A -matrix is

$$A(t) = \begin{bmatrix} \frac{\partial \dot{x}}{\partial x} & \frac{\partial \dot{x}}{\partial y} & \frac{\partial \dot{x}}{\partial z} & \frac{\partial \dot{x}}{\partial p_x} & \frac{\partial \dot{x}}{\partial p_y} & \frac{\partial \dot{x}}{\partial p_z} \\ \frac{\partial \dot{y}}{\partial x} & \ddots & & & & \vdots \\ \frac{\partial \dot{z}}{\partial x} & & \ddots & & & \vdots \\ \frac{\partial \dot{p}_x}{\partial x} & & & \ddots & & \vdots \\ \frac{\partial \dot{p}_y}{\partial x} & & & & \ddots & \vdots \\ \frac{\partial \dot{p}_z}{\partial x} & \dots & \dots & \dots & \dots & \frac{\partial \dot{p}_z}{\partial p_z} \end{bmatrix} = \begin{bmatrix} 0 & 1 & 0 & 1 & 0 & 0 \\ -1 & 0 & 0 & 0 & 1 & 0 \\ 0 & 0 & 0 & 0 & 0 & 1 \\ A_{41} & A_{42} & A_{43} & 0 & 1 & 0 \\ A_{51} & A_{52} & A_{53} & -1 & 0 & 0 \\ A_{61} & A_{62} & A_{63} & 0 & 0 & 0 \end{bmatrix} \quad (25)$$

where

$$\begin{aligned} A_{41} = \frac{\partial \dot{p}_x}{\partial x} &= 1 - \frac{(1-\mu)}{r_1^3} + \frac{3(1-\mu)(x-\mu)^2}{r_1^5} - \frac{\mu}{r_2^3} + \frac{3\mu(x+1-\mu)^2}{r_2^5} \\ A_{52} = \frac{\partial \dot{p}_y}{\partial y} &= 1 - \frac{(1-\mu)}{r_1^3} + \frac{3(1-\mu)y^2}{r_1^5} - \frac{\mu}{r_2^3} + \frac{3\mu y^2}{r_2^5} \\ A_{63} = \frac{\partial \dot{p}_z}{\partial z} &= -\frac{(1-\mu)}{r_1^3} + \frac{3(1-\mu)z^2}{r_1^5} - \frac{\mu}{r_2^3} + \frac{3\mu z^2}{r_2^5} \\ A_{51} = A_{42} = \frac{\partial \dot{p}_x}{\partial y} &= \frac{3(1-\mu)(x-\mu)y}{r_1^5} + \frac{3\mu(x+1-\mu)y}{r_2^5} \\ A_{61} = A_{43} = \frac{\partial \dot{p}_x}{\partial z} &= \frac{3(1-\mu)(x-\mu)z}{r_1^5} + \frac{3\mu(x+1-\mu)z}{r_2^5} \\ A_{62} = A_{53} = \frac{\partial \dot{p}_y}{\partial z} &= \frac{3(1-\mu)yz}{r_1^5} + \frac{3\mu yz}{r_2^5} \end{aligned} \quad (26)$$

We now introduce the square matrix, $\Phi(t, t_0)$, which is made up of $N = 6$ columns (each of which independently satisfies Eq (24)). $\Phi(t, t_0)$ is called the *state transition matrix*

and it maps changes in the initial conditions to changes in the final conditions through the relationship

$$\delta \bar{x}(t) = \Phi(t, t_0) \delta \bar{x}(t_0) \quad (27)$$

Φ therefore satisfies the *equations of variation* which now take the form

$$\dot{\Phi}(t, t_0) = A(t) \Phi(t, t_0) \quad (28)$$

where the initial condition, $\Phi(t_0, t_0)$, equals the identity matrix (I).

3.2.2 Our Periodic Orbit

We now have the necessary tools to find the periodic orbit for our system. The setup for our periodic orbit is shown on Figure 2. It is a symmetric periodic orbit with zero inclination, therefore we set:

$$\begin{aligned} x(0) &= \text{specified} & p_x(0) &= 0 \\ y(0) &= 0 & p_y(0) &= \text{specified} \\ z(0) &= 0 & p_z(0) &= 0 \end{aligned} \quad (29)$$

Although the moon's motion is not, in reality, completely confined to the plane of the primaries' motion, we'll let it be so for the periodic orbit and use other techniques to handle the out-of-plane motion. This assumption was also made by Hill.

The period of the moon in the restricted problem is calculated from a real ephemeris as

$$\tau = 2\pi \frac{\tau_{\text{moon}}}{\tau_{\text{year}}} = 2\pi \frac{29.530589}{365.256363} \quad (30)$$

where τ_{year} is the period of the sidereal year and τ_{moon} is the mean period from new moon to new moon as tabulated in the *Astronomical Almanac* (U.S. Naval Observatory, 1986:C1,D2).

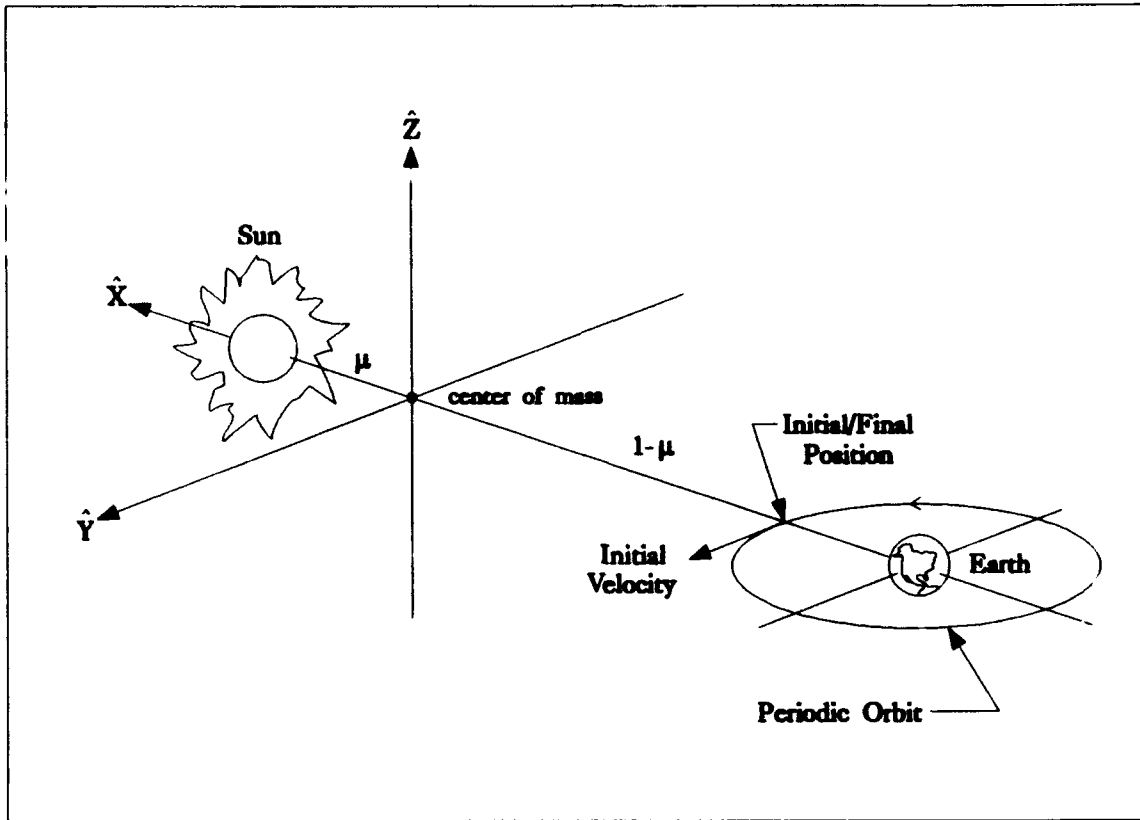


Figure 2. Periodic Orbit in the Restricted Three Body Problem.

At this point, we also determine a value for the parameter μ :

$$\mu = m_2 = \frac{M_2}{M_1 + M_2} = 3.00348069 \times 10^{-6} \quad (31)$$

Here, $M_1 = 1$, and $M_2 = 1/332,946.038$ solar masses (U.S. Naval Observatory, 1986:K6).

The general approach is to start with a guess for the initial conditions based on two-body dynamics and iteratively integrate the state vector and Φ matrix forward in time to one period using the EOM/EOV until Eq (20) is satisfied.. Specifically, we want $y(0) = y(\tau) = 0$ and $p_x(0) = p_x(\tau) = 0$. z and p_z will stay at zero by themselves, and x and p_y will return to their initial values due to symmetry as long as y and p_x return to zero. After each integration, the error at $t = \tau$ is simply:

$$\bar{e} = \begin{pmatrix} y(\tau) \\ p_x(\tau) \end{pmatrix} \quad (32)$$

So the correction to the final state is just $-\bar{e}$. Now we want to know how to change the initial conditions to effect the corrections in the final conditions. Using Eq (27), and removing all of the superfluous elements, we have:

$$\delta \bar{x}(\tau) = \Phi(\tau, 0) \delta \bar{x}(0)$$

$$-\begin{pmatrix} y(\tau) \\ p_x(\tau) \end{pmatrix} = \begin{Bmatrix} \Phi_{21} & \Phi_{25} \\ \Phi_{41} & \Phi_{45} \end{Bmatrix} \begin{pmatrix} \delta x(0) \\ \delta p_y(0) \end{pmatrix} \quad (33)$$

By solving for $\delta \bar{x}(0)$, we find the corrections to the initial conditions. Those corrections are added and the process is started again. This is done iteratively until some tolerance is met (we used 10^{-10}).

3.2.3 First Guess for Initial Conditions

To get our first pass guess for initial conditions, we used two body dynamics solutions. As shown in Figure 3, the initial x position in the restricted three body coordinates component is

$$x_0 = -\left((1-\mu) - \frac{R_{moon}}{1\text{AU}} \right)$$

$$x_0 = -\left((1-\mu) - \frac{385,000 \text{ km}}{1.4959787 \times 10^8 \text{ km}} \right) = -.997423 \text{ AU} \quad (34)$$

while the initial y velocity component (in R3B coordinates) is

$$\dot{y}_0 = \sqrt{\frac{\mu_{\oplus}}{R_{moon}}}$$

$$\dot{y}_0 = \sqrt{\frac{3.986012 \times 10^5 \frac{\text{km}^3}{\text{s}^2}}{385,000 \text{ km}}} = 1.0175 \frac{\text{km}}{\text{s}} = .034162 \frac{\text{AU}}{\text{TU}} \quad (35)$$

where μ_{\oplus} is the gravitational parameter for the earth and R_{moon} is the approximate mean radius of the moon with respect to earth's center. But since we need the *momentum* in the y -direction, we use the equations of motion to get

$$p_{y0} = \dot{y}_0 + x_0 = -.963261 \quad (36)$$

This gives us the first guess for the initial conditions which looks like this:

$$\bar{x}(0) = [-.997423 \ 0 \ 0 \ 0 \ -.963261 \ 0]^T \quad (37)$$

After doing the iterative corrections, the final result is the initial condition state vector for our periodic orbit

$$\bar{x}_p(0) = [-.997456 \ 0 \ 0 \ 0 \ -.965393 \ 0]^T \quad (38)$$

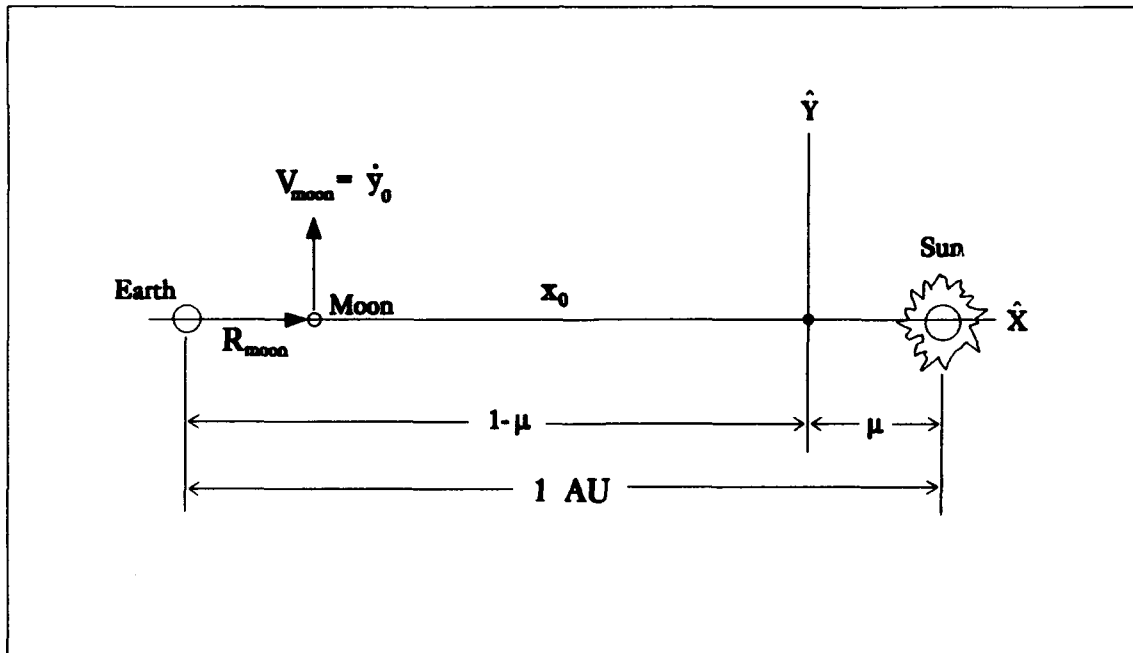


Figure 3. Two Body Initial Guess in the Restricted Three Body Coordinates.

3.3 Classical Floquet Theory

The basic contribution of classical Floquet theory is that the periodic state transition matrix, Φ , can be written as

$$\Phi(t, t_0) = F(t) e^{J(t-t_0)} F^{-1}(t_0) \quad (39)$$

where F is a periodic matrix, and J is a constant matrix of system frequencies in Jordan normal form. These system frequencies are called Poincaré exponents. If we can find the constant J matrix, as well as the F matrix over one period, then we have Φ over one period and, therefore, we have Φ for all time.

To determine J and F , the equations of variation (Eq (28)) are integrated forward in time to one period (τ). Conveniently, this was already done in the last iteration of finding our periodic orbit (§3.2.2). The result is $\Phi(\tau, 0)$, called the *monodromy matrix*, which looks like

$$\Phi(\tau, 0) = F(\tau) e^{J\tau} F^{-1}(0) \quad (40)$$

But $F(\tau) = F(0)$ because F is periodic, so

$$\Phi(\tau, 0) = F(0) e^{J\tau} F^{-1}(0) \quad (41)$$

After rearranging, we get

$$F^{-1}(0) \Phi(\tau, 0) F(0) = e^{J\tau} \quad (42)$$

which shows that $F(0) = F(\tau)$ is the matrix of eigenvectors of $\Phi(\tau, 0)$, and $e^{J\tau}$ is the diagonal matrix of eigenvalues of $\Phi(\tau, 0)$. Therefore, after finding the monodromy matrix, the next step is to find its eigenvalues and eigenvectors.

Given the constant eigenvalues, λ_i , for the system, then from Eq (42)

$$\lambda_i = e^{\omega_i \tau} \quad (43)$$

where ω_i are the system frequencies (Poincaré exponents). Solving for ω_i yields

$$\omega_i = \frac{1}{\tau} \ln \lambda_i \quad (44)$$

which are the constant diagonal values of the J matrix. These Poincaré exponents always occur as positive/negative pairs for canonical systems (each pair corresponding to a mode), with one exception: when $\lambda_i = 1$, then there is a repeated value of $\omega_i = 0$. We call this pair of zeroes a *degenerate mode*. For each of these degenerate mode pairs, there is an exact integral of motion, and a value of one appears in the off-diagonal region of J . It is also noteworthy that the Poincaré exponents give important linear stability information about the periodic orbit. They "can be interpreted just like the eigenvalues of a constant coefficient system. The imaginary part of ω_i is the oscillatory frequency of the mode i , while a positive real part indicates instability" (Wiesel, 1993:125). For our specific periodic orbit, we get one degenerate mode and two purely imaginary modes. Because the Poincaré exponents have no real parts

$$\begin{aligned}\omega_1 &= 0 + 0i \\ \omega_2 &= 0 + 0.8853941825307i \\ \omega_3 &= 0 + 1.053464567610i \\ \omega_4 &= 0 + 0i \\ \omega_5 &= 0 - 0.8853941825307i \\ \omega_6 &= 0 - 1.053464567610i\end{aligned}$$

we know the system is stable. The monodromy matrix $\Phi(\tau, 0)$, initial eigenvector matrix $F(0)$, and J matrix are shown in Appendix A.

The next step is to get the eigenvector matrix, $F(t)$, over one period. Using Floquet's Theorem (Eq (39)) and differentiating, we find

$$\begin{aligned}\Phi(t, t_0) &= F(t)e^{J(t-t_0)}F^{-1}(t_0) \\ \dot{\Phi}(t, t_0) &= \dot{F}(t)e^{J(t-t_0)}F^{-1}(t_0) + F(t)Je^{J(t-t_0)}F^{-1}(t_0)\end{aligned}$$

So, by substituting into Eq (28)

$$\dot{\Phi}(t, t_0) = A(t)\Phi(t, t_0)$$

$$\dot{F}(t)e^{J(t-t_0)}F^{-1}(t_0) + F(t)Je^{J(t-t_0)}F^{-1}(t_0) = A(t)F(t)e^{J(t-t_0)}F^{-1}(t_0)$$

$$\dot{F}(t) + F(t)J = A(t)F(t)$$

Therefore,

$$\dot{F} = AF - FJ \quad (45)$$

is a differential equation for $F(t)$. With the initial condition, $F(0)$, already known, we can integrate from $t = 0 \rightarrow \tau$ to get $F(t)$ over one period, which can be reduced into a series of Fourier coefficients as described by Brouwer and Clemence (1961:108-113).

By knowing $F(t)$ over one period, we also have a coordinate transformation from physical variables, $\delta\bar{x}$, to modal variables, \bar{y}

$$\bar{y}(t) \equiv F^{-1}(t)\delta\bar{x}(t) \quad (46)$$

which is derived from equation (27) by

$$\delta\bar{x}(t) = \Phi(t, t_0)\delta\bar{x}(t_0)$$

$$\delta\bar{x}(t) = F(t)e^{J(t-t_0)}F^{-1}(t_0)\delta\bar{x}(t_0)$$

$$F^{-1}(t)\delta\bar{x}(t) = e^{J(t-t_0)}F^{-1}(t_0)\delta\bar{x}(t_0)$$

$$\bar{y}(t) = e^{J(t-t_0)}\bar{y}(t_0) \quad (47)$$

Equation (47) is the modal coordinate form of the Floquet Solution. It is a solution to the linear, constant coefficient, modal equation:

$$\dot{\bar{y}} = J\bar{y} \quad (48)$$

where, for canonical systems, J has the form $J = ZS$, S being a symmetric matrix.

Classical Floquet theory gives us a complete solution (Eq (39)) to the EOVS, stability information, and a transformation to modal coordinates (Eq (46)). To do the perturbation expansion discussed in a later section, it is necessary that the transformation be canonical.

3.4 Canonical Floquet Theory

In the last section, we defined the transformation to modal coordinates as

$$\bar{y}(t) \equiv F^{-1}(t) \delta \bar{x}(t) \quad (46)$$

We would like this modal transformation to be canonical so that a new Hamiltonian can be derived for the perturbation expansion analysis in a later section.

The transformation above is canonical only if $F(t)$ is a *symplectic* matrix. That is

$$Z = F^T Z F \quad (49)$$

must hold for all time where Z is the correlation matrix. This ensures that the new modal Hamiltonian, $\mathcal{K}(\bar{y})$, follows Hamilton's equations (Eq (21))

$$\dot{\bar{y}} = Z \frac{\partial \mathcal{K}(\bar{y})}{\partial \bar{y}} \quad (50)$$

where \bar{y} is the *modal* state vector.

An algorithm was presented by Siegel and Moser (1971:97-103) that normalizes $F(0)$ to a symplectic matrix, but this algorithm only accounted for a constant F matrix and a non-degenerate case. Later, Wiesel and Pohlen (1992:6-12) expanded the utility of this algorithm to include periodic F matrices and degenerate modes.

3.4.1 Symplectic Periodicity for Non-Degenerate Modes

Because the Poincaré exponents, ω_i , always occur in positive/negative pairs for non-degenerate canonical systems, the J matrix can be written in the form

$$J = \begin{Bmatrix} \Omega & 0 \\ 0 & -\Omega \end{Bmatrix} \quad (51)$$

where Ω is a diagonal matrix with one of each ω_i pair on the diagonal. By differentiating Eq (49) and recognizing that Z is constant matrix, we get

$$\dot{Z} = \dot{F}^T Z F + F^T Z \dot{F} = 0 \quad (52)$$

Substituting Eq (45) and Eq (49) and some correlation matrix identities, this can be rearranged to obtain

$$-J^T Z - Z J = 0 \quad (53)$$

which proves to be true since

$$-J^T Z - Z J = \begin{Bmatrix} 0 & -\Omega \\ -\Omega & 0 \end{Bmatrix} + \begin{Bmatrix} 0 & \Omega \\ \Omega & 0 \end{Bmatrix} = 0 \quad (54)$$

Therefore, if $F(0)$ can be made symplectic, then $F(t)$ will stay symplectic for all time (Wiesel and Pohlen, 1992:7).

3.4.2 Symplectic Periodicity for Degenerate Modes

For systems with a degenerate mode, the J matrix will have a pair zeros and take the form

$$J = \begin{Bmatrix} \Omega & \Psi \\ 0 & -\Omega \end{Bmatrix} \quad (55)$$

where Ψ has a 1 on its diagonal location that occupies the same row/column as the degenerate mode and zeros everywhere else. Just as with the non-degenerate case, we substitute J into Eq (53) to show that

$$-J^T Z - Z J = \begin{Bmatrix} 0 & -\Omega \\ -\Omega & -\Psi \end{Bmatrix} + \begin{Bmatrix} 0 & \Omega \\ \Omega & \Psi \end{Bmatrix} = 0 \quad (56)$$

So, once again, the same *starts symplectic, stays symplectic* theory holds true. The next step is to actually make the initial eigenvector matrix symplectic: the subject discussed in the next section.

3.5 Symplectic Normalization

The theory for symplectic normalization is presented in detail by Wiesel and Pohlen (1992:8-12), and discusses all possible cases. This section only summarizes the method as it applies to the lunar modes; that is, one degenerate mode and two non-degenerate (pure imaginary) modes.

Right now, we have the eigenvector matrix (F) of Φ which follows from Floquet's Theorem. The intent is to get another eigenvector matrix (E) which solves this equation

$$E^{-1}\Phi E = e^{J\tau} \quad (57)$$

and at the same time is symplectic.

$$Z = E^T Z E \quad (58)$$

We can write the relationship of the two eigenvector matrices as

$$E = F D \quad (59)$$

where

$$D = \begin{bmatrix} d_1 & c \\ 0 & d_2 \end{bmatrix} \quad (60)$$

Matrices d_1 and d_2 are diagonal matrices of multiplicative scale factors. These scale factors are arbitrary with the constraint that the i th entries in d_1 and d_2 corresponding to repeated eigenvalues (degenerate mode) be the same. The matrix c is zero everywhere unless there is a degenerate mode, in which case there is a 1 in the i th entry along the diagonal corresponding to the degenerate mode. In our particular case, there is a degenerate mode, so all of the caveats apply.

Substituting Eq (59) into Eq (58) and rearranging, we get

$$D^{-T} Z D^{-1} = F^T Z F \quad (61)$$

where D^{-T} is the inverse of the transpose of D . By direct calculation, the above equation becomes

$$D^{-T} Z D^{-1} = \begin{bmatrix} 0 & d_1^{-1} d_2^{-1} \\ -d_1^{-1} d_2^{-1} & 0 \end{bmatrix} = F^T Z F \quad (62)$$

Since we know F , we can determine the product $d_1 d_2$. By setting $d_1 = d_2$ as suggested by Wiesel and Pohlen, we can solve for the diagonal entries of d_1 and d_2 by

$$d_{1,\mu} = d_{2,\mu} = \frac{1}{\sqrt{(F^T Z F)_{i,j+N}}} \quad (63)$$

With the diagonal values of the D matrix calculated, equation (59) returns the symplectically normalized initial eigenvector matrix E .

3.5.1 Generalized Eigenvectors

As mentioned before, our periodic orbit has a degenerate mode, which means one of the eigenvectors (\tilde{f}_4) in the F matrix is not linearly independent. To continue, we need a generalized eigenvector (\tilde{f}_4') before normalizing to the E matrix. To get our generalized eigenvector, we need to look at the form of the conjugate eigenvector for the degenerate mode

$$\tilde{f}_1 = [0 \quad f_2 \quad 0 \quad f_4 \quad 0 \quad 0]^T \quad (64)$$

We want linear independence, so if we choose \tilde{f}_4' to have the form

$$\tilde{f}_4' = [f_1' \quad 0 \quad 0 \quad 0 \quad f_5' \quad 0]^T \quad (65)$$

then perpendicularity between the two is automatic.

$$\tilde{f}_1 \cdot \tilde{f}_4' = 0 \quad (66)$$

The generalized eigenvector is now calculable from

$$(\Phi - I) \tilde{f}_4' = \tau \tilde{f}_1 \quad (67)$$

where τ is the period of the periodic orbit and specific to canonical problems. Without the factor of τ included, the F (or E) matrix is not periodic.

3.6 Modal Variable Development

We have the initial state vector for the periodic orbit in physical variables, $\bar{x}_p(0)$, as well as the initial symplectically normalized eigenvector matrix $E(0)$. Using equations of motion found earlier

$$\dot{\bar{x}}_p = Z \frac{\partial \mathcal{H}}{\partial \bar{x}_p} \quad (21)$$

$$\dot{E} = AE - EJ \quad (45)$$

the two are integrated forward in time to one period. As both are periodic, they can be reduced to Fourier series coefficients by harmonic analysis. The method for harmonic analysis is shown in Brouwer and Clemence (1961:108-113), although we use an exponential form instead of the sin/cosine form to accommodate the complex valued E matrix. With these Fourier coefficients, we know $\bar{x}_p(t)$ and $E(t)$ for all time.

The next step is to randomly select an initial condition state vector, $\bar{x}(0)$, for a near-periodic orbit trajectory, and integrate forward in evenly spaced time steps through one period. At each time step, the periodic state vector and E matrix are derived from their Fourier coefficients as

$$\bar{x}_p(t) = \sum_{j=-\infty}^{j=\infty} (gx)_j e^{j\omega t}$$

$$\bar{E}(t) = \sum_{j=-\infty}^{j=\infty} (ge)_j e^{j\omega t}$$

where gx and ge are the Fourier coefficients and i is the imaginary value $\sqrt{-1}$. The variation in physical variables $\delta\bar{x}(t)$ is also calculated at each time

$$\delta\bar{x}(t) = \bar{x}(t) - \bar{x}_p(t) \quad (68)$$

which is finally transformed to modal variables using the now familiar relation

$$\bar{y}(t) = E^{-1}(t) \delta\bar{x}(t) \quad (69)$$

Remember that the E matrix replaces the F matrix for a canonical transformation.

We now have the modal coordinate form of the Floquet solution to any orbit that is near our periodic orbit. The form of these modal variables is special. For the non-degenerate modes, an unusual symmetry exists between the conjugate modal variables, y_i and y_{i+N} : their real/imaginary parts are switched and of the opposite sign. For example,

$$\begin{array}{ccc} y_i = -a + bi & & y_i = -a - bi \\ y_{i+N} = -b + ai & \text{or} & y_{i+N} = +b + ai \end{array}$$

For degenerate modes, the real parts are always zero, and the conjugate imaginary parts are independent.

$$\begin{array}{l} y_i = 0 + ci \\ y_{i+N} = 0 + di \end{array}$$

All in all, there are only two unique values to plot for each pair of conjugate modal variables. For the non-degenerate modes, we plot the real vs. imaginary parts of the modal variables to get phase portraits. There only needs to be one plot for each conjugate pair due to the symmetry (i.e. pick y_i or y_{i+N}). For the degenerate modes, we plot the imaginary parts of the of the conjugate y_i , y_{i+N} variables. In the linear regime of the periodic orbit, these phase portraits have the characteristic forms of centers, saddle points, and straight lines. The centers arise from modes corresponding to purely imaginary Poincaré exponents, the saddles from modes with real Poincaré exponents, and the straight lines from degenerate modes (zero Poincaré exponents). For our periodic orbit case, there are two modes with purely imaginary Poincaré exponents and one degenerate mode. As long as we stay in the linear regime, the three plots should nominally show two circles and one line.

The behavior of the three modes maps back to classical orbital characteristics in the physical variables. For the degenerate mode (mode 1), variable y_1 corresponds to a time displacement of the periodic orbit, while y_4 corresponds to negative energy (Wiesel, 1981:236; Wiesel, 1993:23). We refer to mode 1 as the *time/energy mode*. Modes 2 and 3 are the vertical and planar modes respectively, which can be observed by looking at the eigenvector matrix F in Appendix A. Vectors 2 and 5 have only vertical components (z and p_z), while

vectors 3 and 6 have no vertical components. The Poincaré exponents (or modal frequencies) of these two modes, "when referenced to inertial space, imply modal periods of 8.725 yr for the planar mode, and 18.703 yr for the vertical mode. These are the familiar periods for the advance of the perigee and regression of the node in the lunar theory." (Wiesel, 1981:588-589) Therefore, we call mode 2 the *inclination mode* and mode 3 the *eccentricity mode*.

To demonstrate the characteristics of these modal plots, we start by picking the near-periodic orbit trajectory to be the actual periodic orbit we found earlier. This should make $\delta\bar{x}(t)$ zero for all time, which makes the modal vector zero as well. The modal plots are simply points with random noise at (0,0) (see Figures 4-6). Next, we excite the modes by perturbing the near-periodic orbit, \bar{x} , to something other than the periodic orbit. This is simply a matter of changing the initial conditions. For illustration purposes, each mode is excited independently with appropriate initial conditions. Figures 7-9 show examples of modal plots from orbit trajectories in the linear regime of the periodic orbit. They are nearly perfect circles (Figures 8 and 9) and a something approaching a straight line (Figure 7) when the initial conditions are perturbed within the linear region. Figures 10-12 show the modes of an orbit well outside the linear regime. They are unstable spirals and erratic oscillations.

In the next section, we want to determine if the actual lunar orbit is legitimately one of the near-periodic orbits. In other words, is the moon's orbit in or near the linear regime of our periodic orbit?

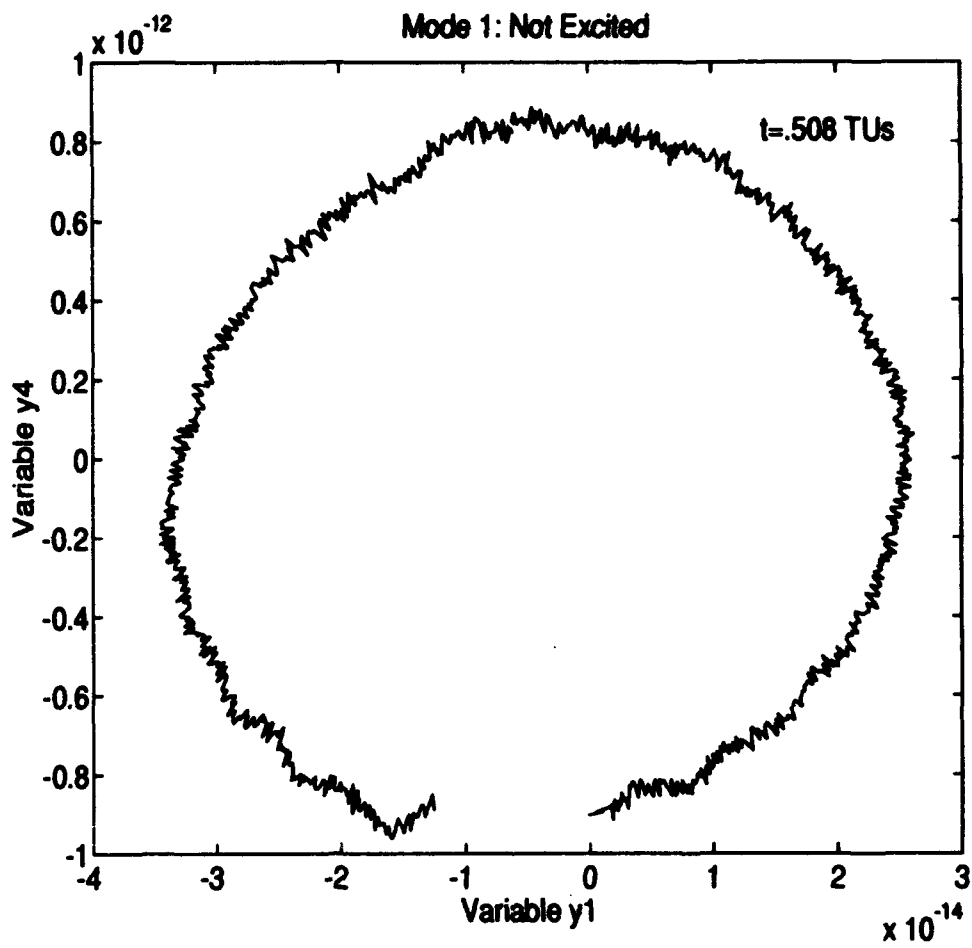


Figure 4. Time/Energy Mode using Periodic Orbit Initial Conditions.

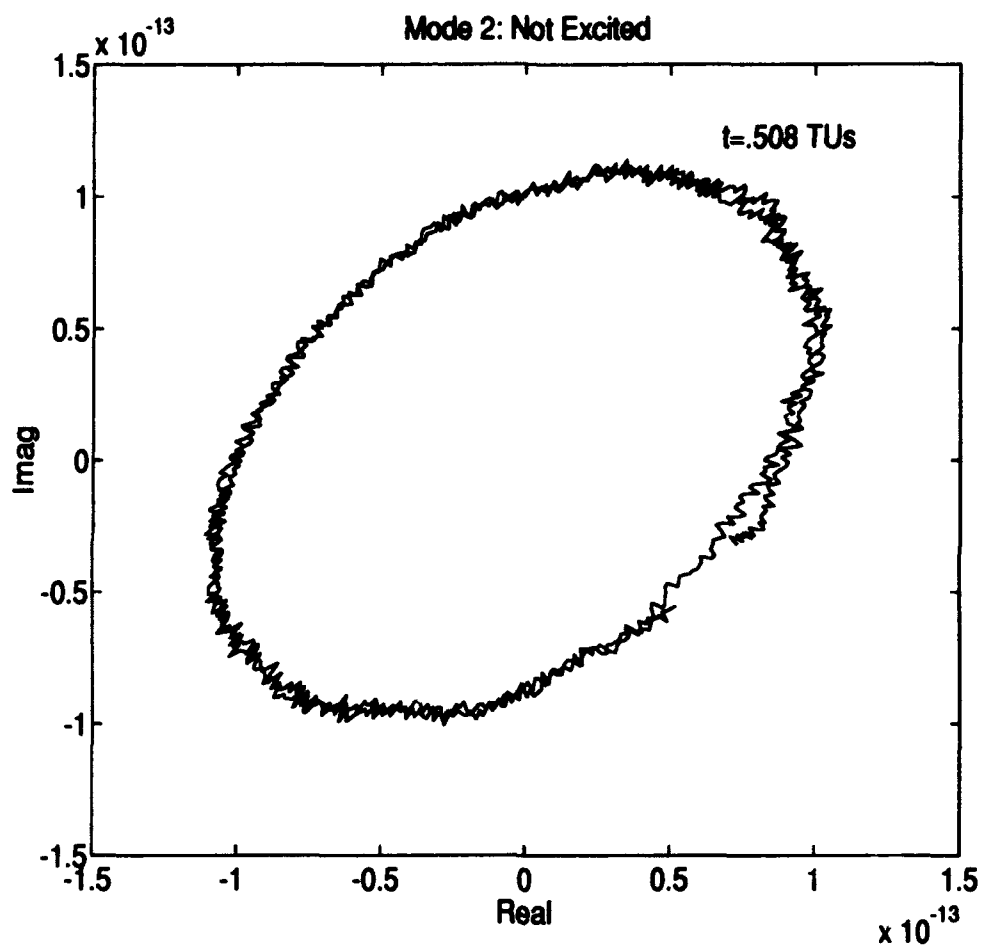


Figure 5. Inclination Mode using Periodic Orbit Initial Conditions.

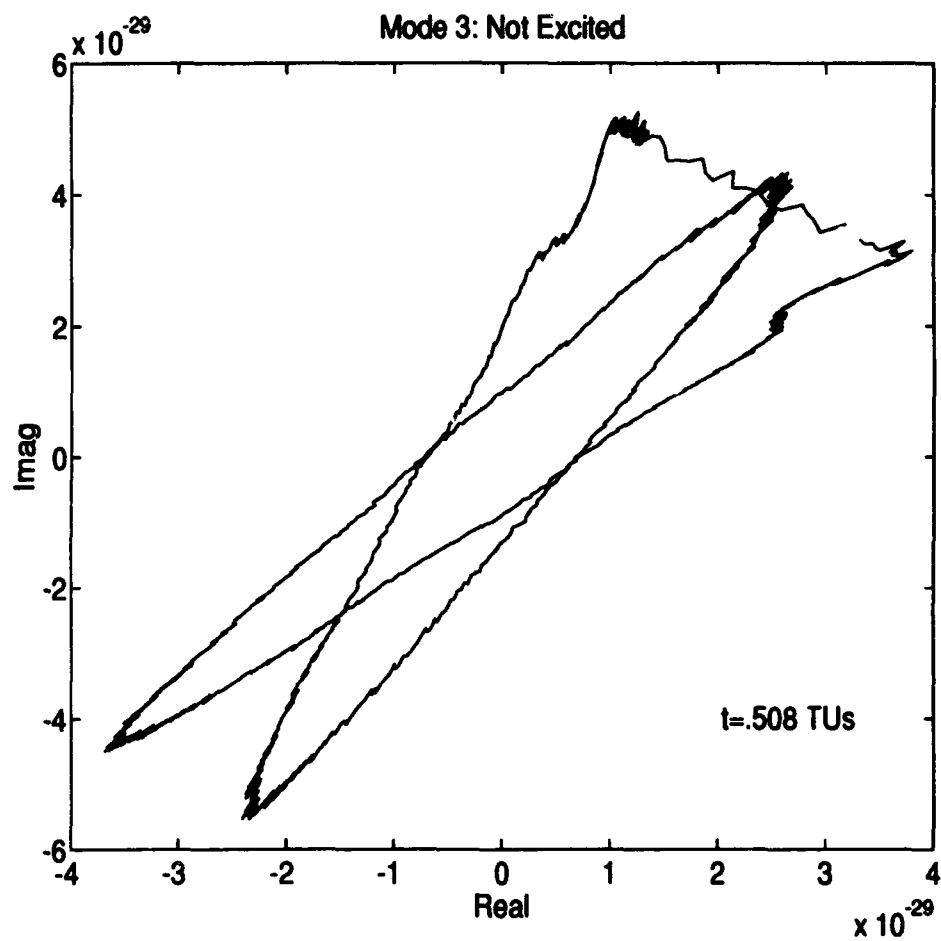


Figure 6. Eccentricity Mode using Periodic Orbit Initial Conditions.

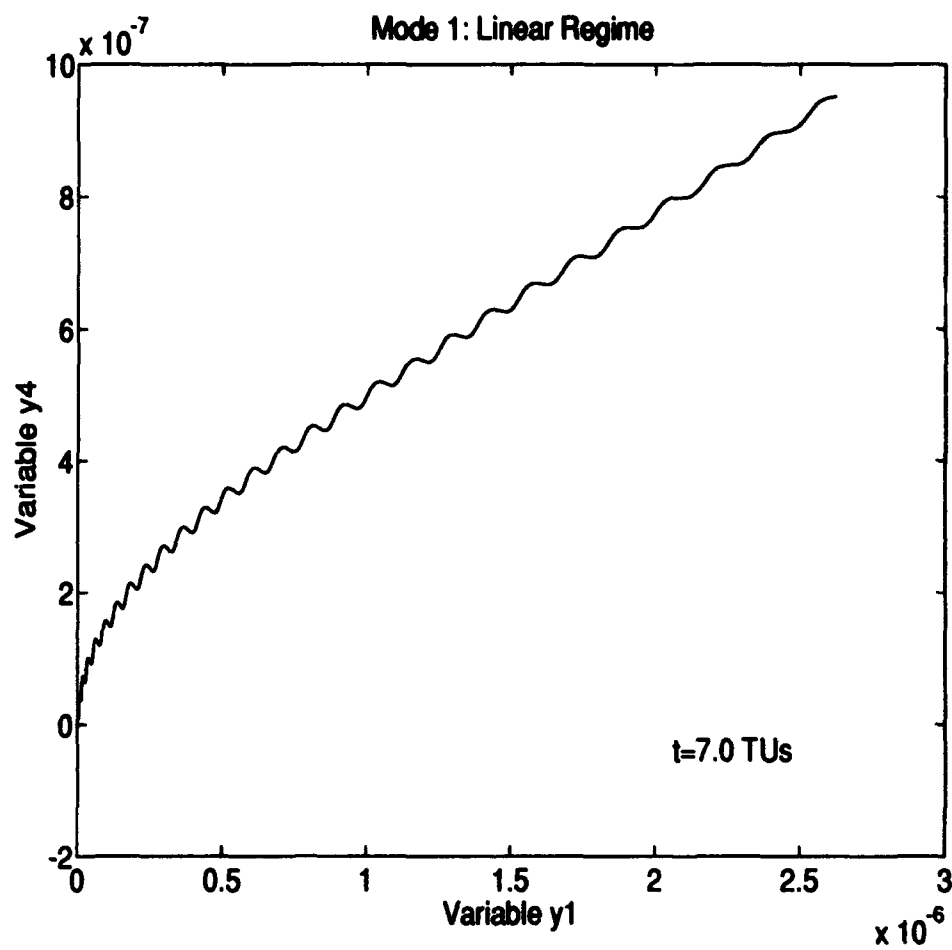


Figure 7. Time/Energy Mode using Initial Conditions in the Linear Region.

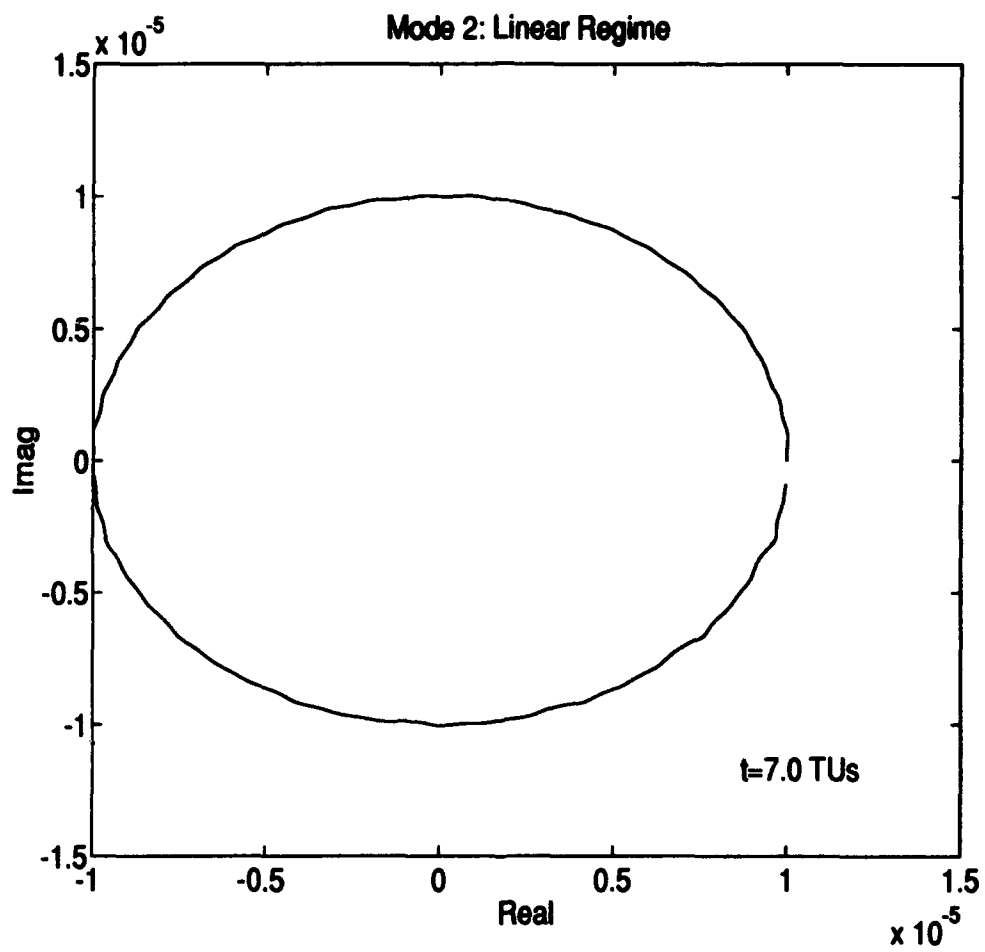


Figure 8. Inclination Mode using Initial Conditions in the Linear Region.

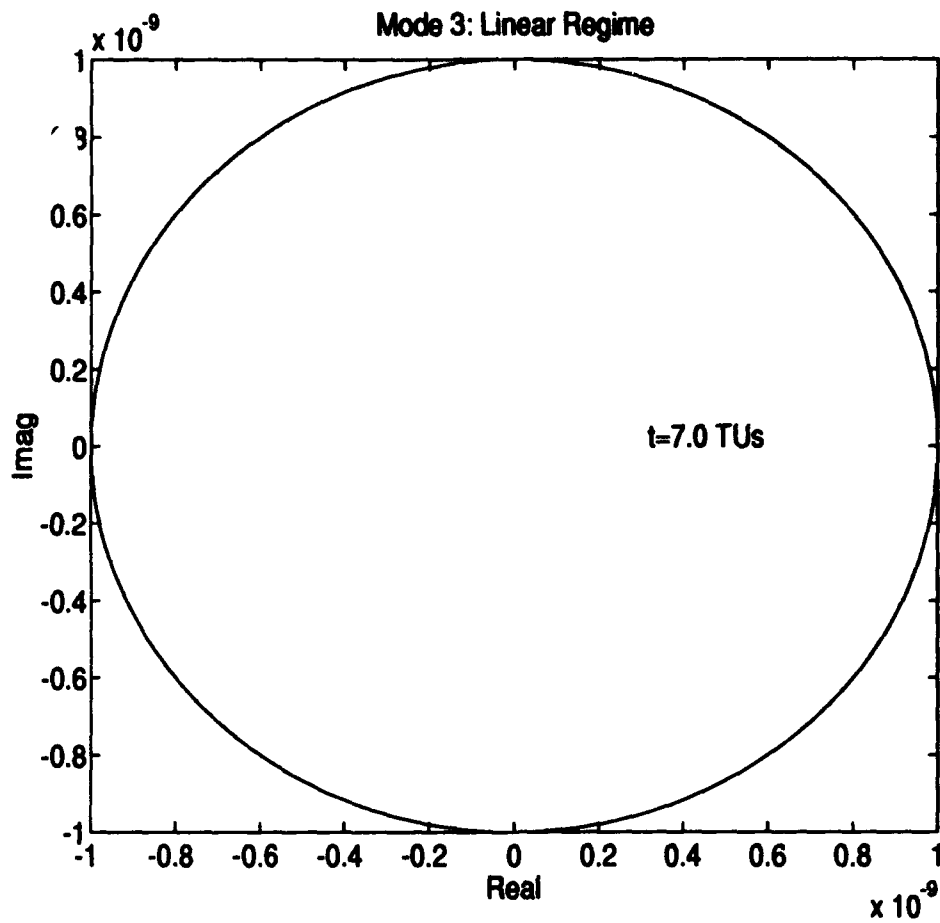


Figure 9. Eccentricity Mode using Initial Conditions in the Linear Region.

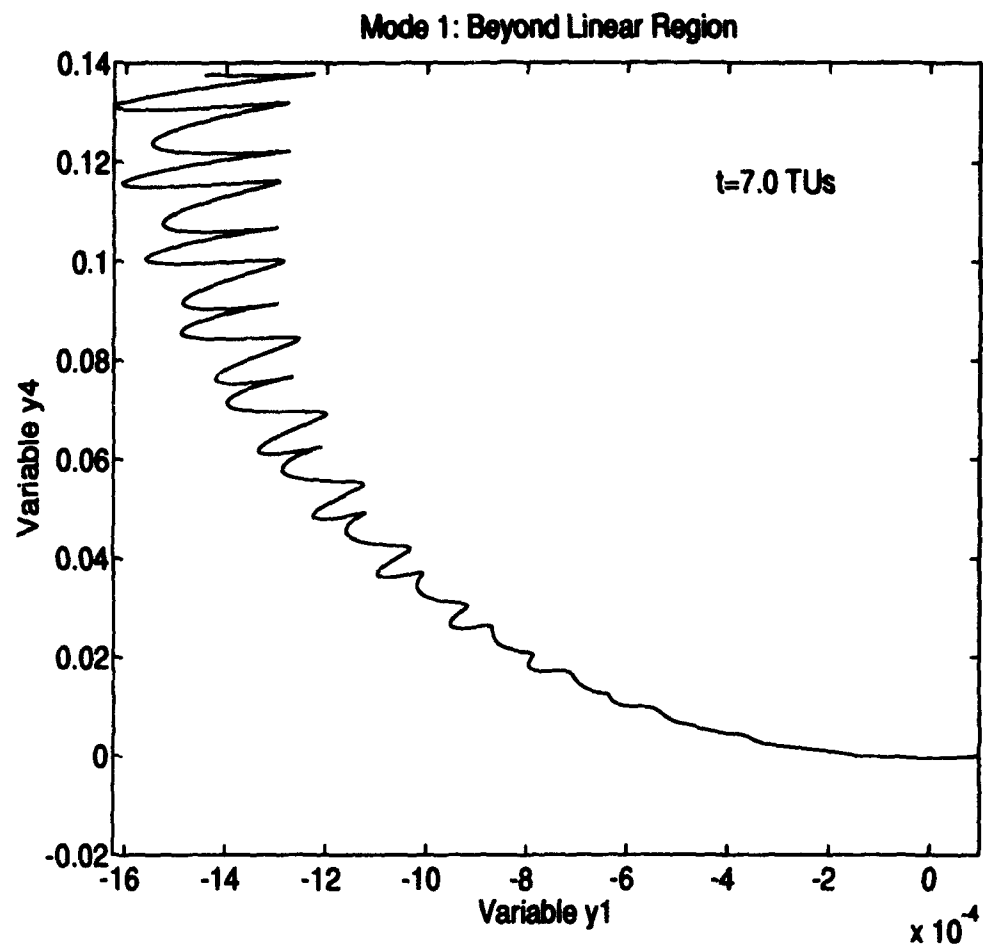


Figure 10. Time/Energy Mode using Initial Conditions Beyond the Linear Region.

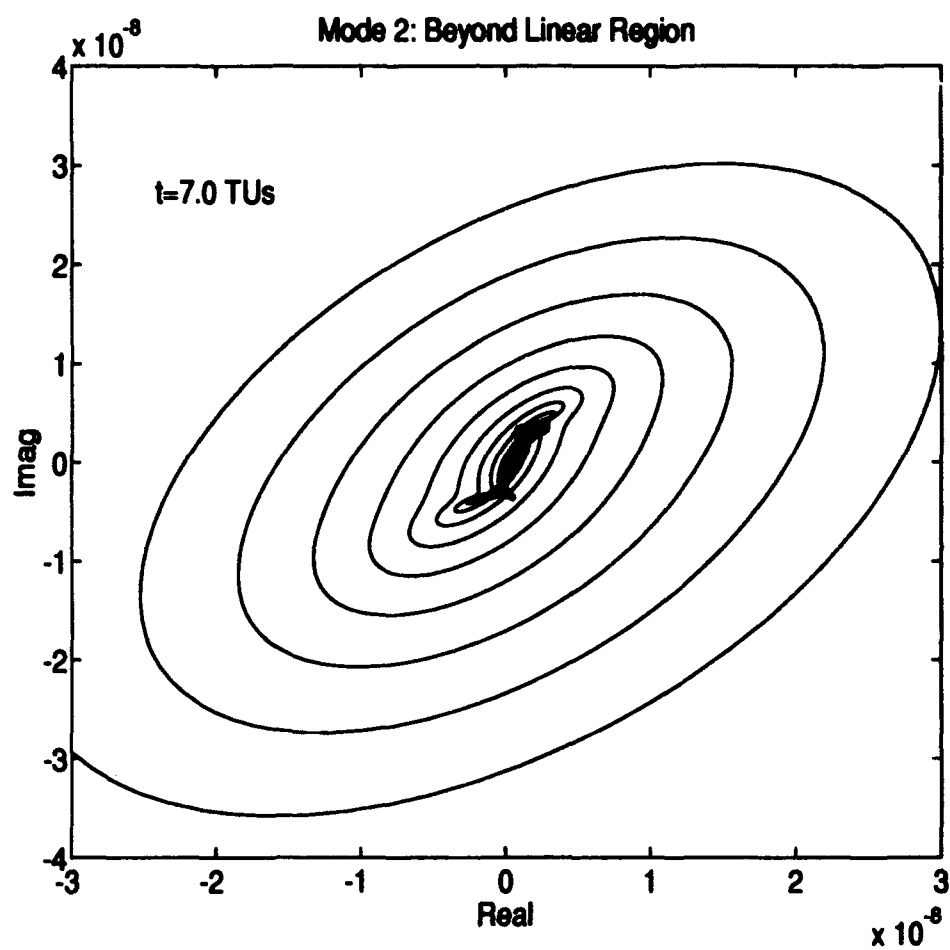


Figure 11. Inclination Mode using Initial Conditions Beyond the Linear Region.

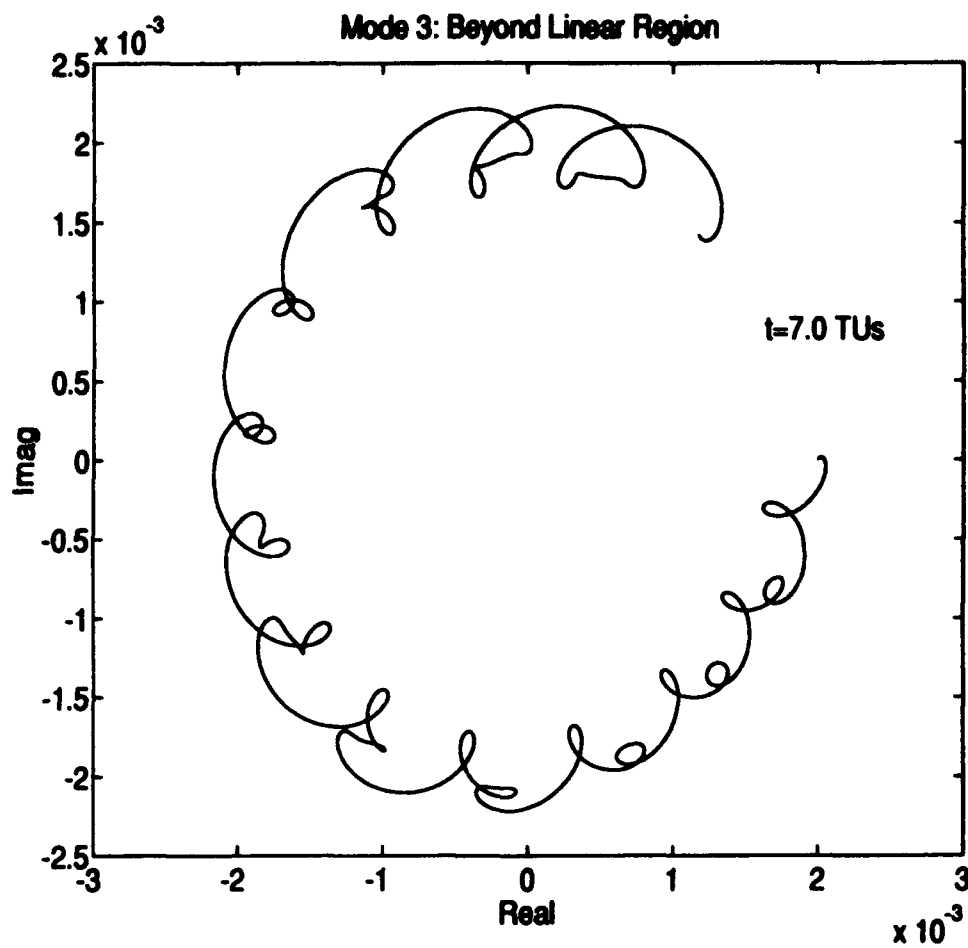


Figure 12. Eccentricity Mode using Initial Conditions Beyond the Linear Region.

3.7 Actual Lunar Orbit

We now want the near-periodic orbit to be the actual moon's orbit. This section discusses the method for using real historical lunar data to get an initial condition state vector, $\bar{x}(0)$, for modal development. With reference to Pohlen (1992), this development is what he would call the "exact representation" of the modal variables.

3.7.1 Getting $\bar{x}(0)$ from the Ephemeris

To begin, we select some random time at which a new moon occurred, and take ephemerides from five evenly spaced times that surround the new moon. Specifically, the following data is collected from the *American Ephemeris and Nautical Almanac* (U.S. Naval Observatory, 1967) at each of the five times:

- lat_m - Apparent Latitude of the Moon with respect to the Ecliptic Plane
- lon_m - Apparent Longitude of the Moon from the Vernal Equinox in the Ecliptic Plane
- Π_m - Horizontal Parallax of the Moon
- lon_s - Longitude of the Sun from the Vernal Equinox in the Ecliptic Plane

The horizontal parallax, shown in Figure 13, translates to a distance, R , between the earth and moon as

$$R = \frac{R_\oplus}{\sin \Pi_m} \quad (70)$$

The data gathered gives information that looks like Figure 14, but what is really needed is the position of the moon with respect to the earth in a coordinate system that rotates with the earth around the sun. Figure 15 shows such a geocentric coordinate system, \hat{b} , whose \hat{b}_1 - \hat{b}_2 plane stays in the ecliptic and whose \hat{b}_1 -axis always points towards the sun. This coordinate frame is referred to as the Earth Centered Rotating (ECR) frame.

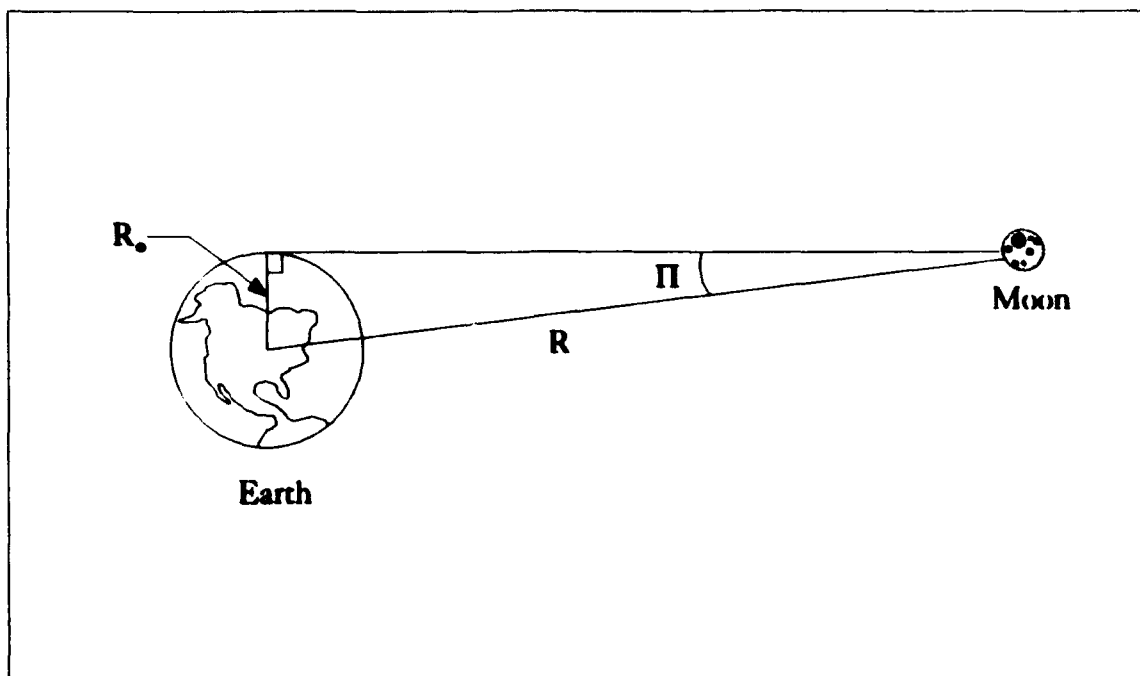


Figure 13. Horizontal Parallax.

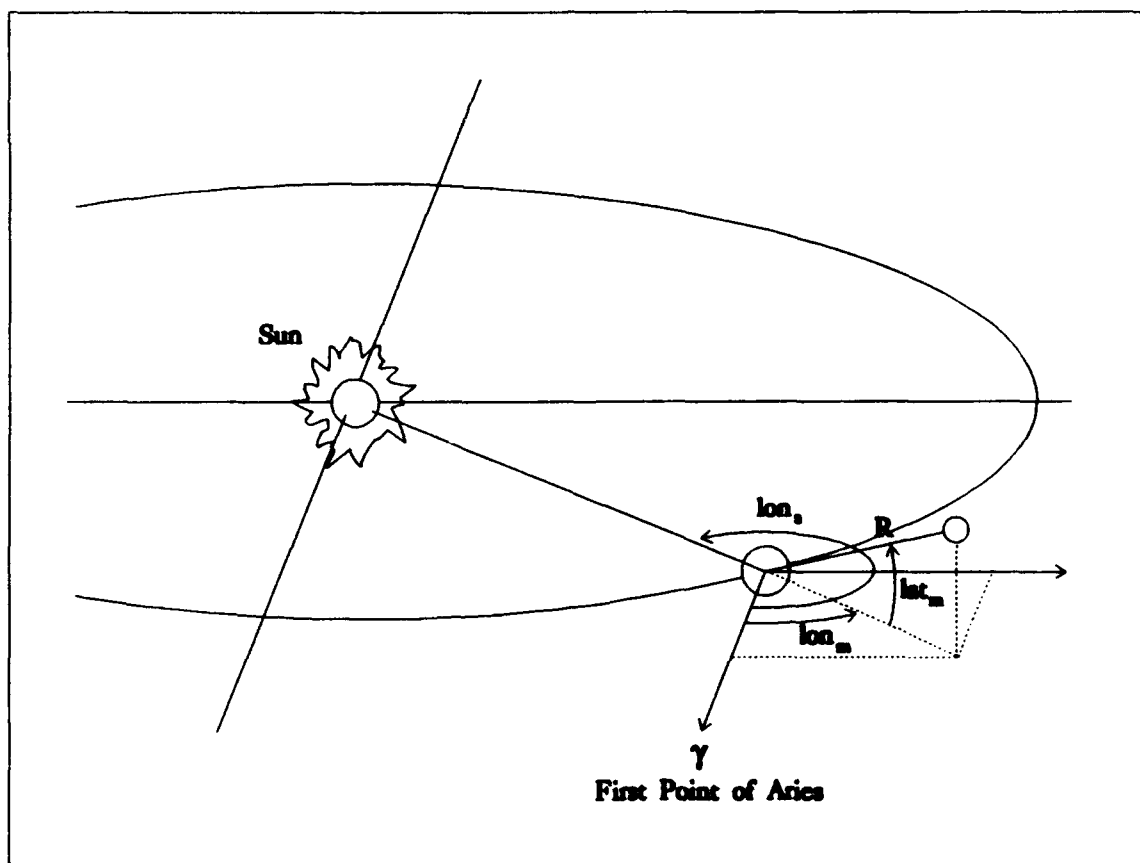


Figure 14. Data Gathered from Ephemerides.

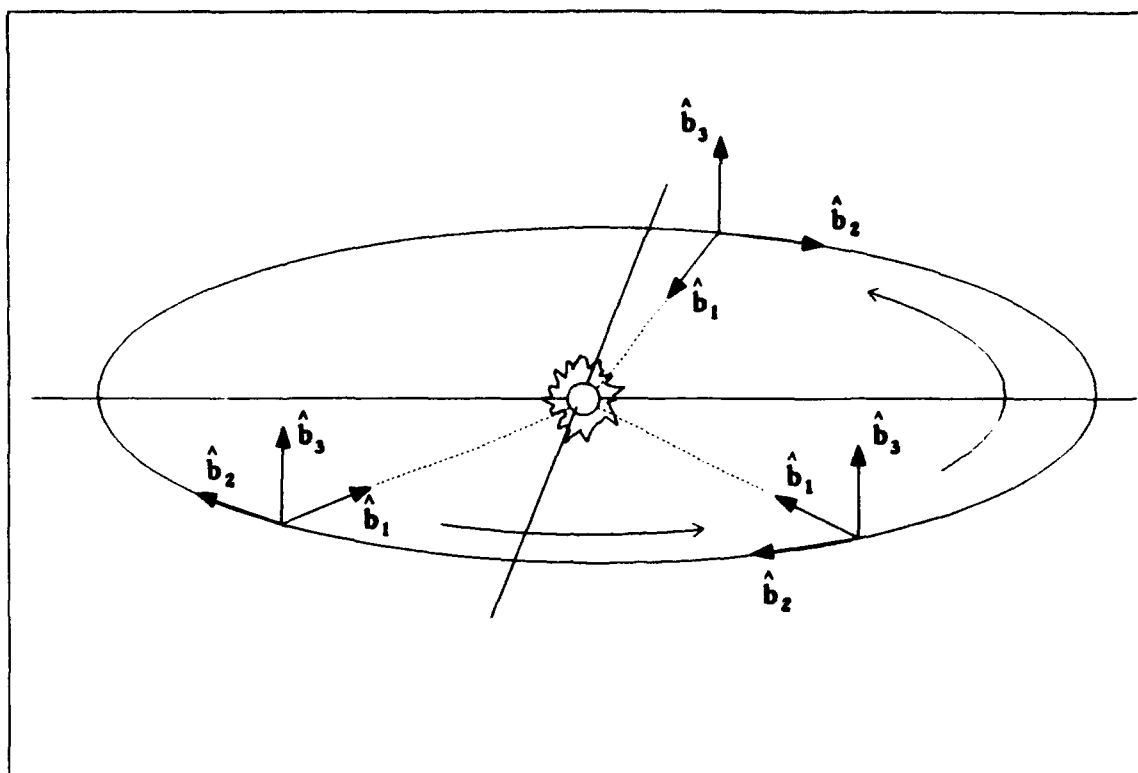


Figure 15. Earth Centered Rotating (ECR) Coordinate Frame.

Subtracting the sun's longitude from the moon's longitude

$$\delta lon_m = lon_m - lon_s \quad (71)$$

yields the desired moon position information with respect to new ECR frame in the polar coordinates: $lat_m, \delta lon_m, R$ (see Figure 16). To get from polar coordinates to rectangular coordinates we use

$$\bar{r}_{ECR} = \begin{bmatrix} x' \\ y' \\ z' \end{bmatrix} = \begin{bmatrix} R \cos(lat_m) \cos(\delta lon_m) \\ R \cos(lat_m) \sin(\delta lon_m) \\ R \sin(lat_m) \end{bmatrix} \quad (72)$$

Figure 17 shows this transformation.

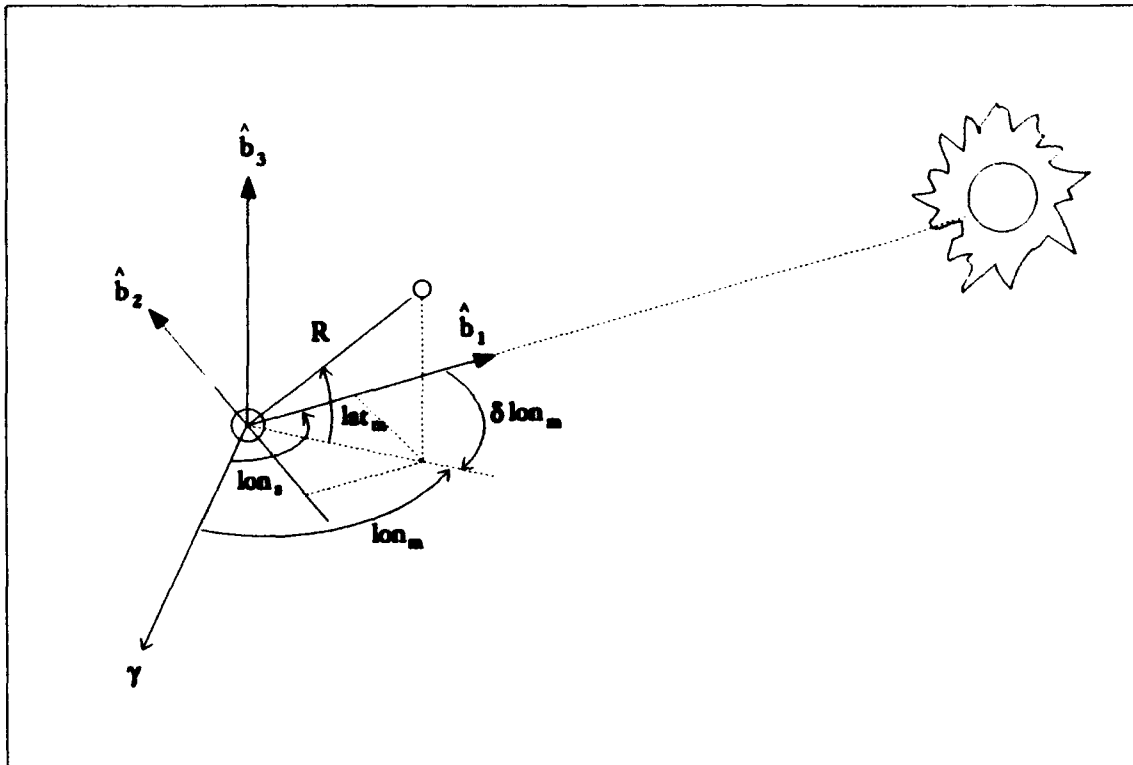


Figure 16. Polar Coordinates Relative to the ECR Frame.

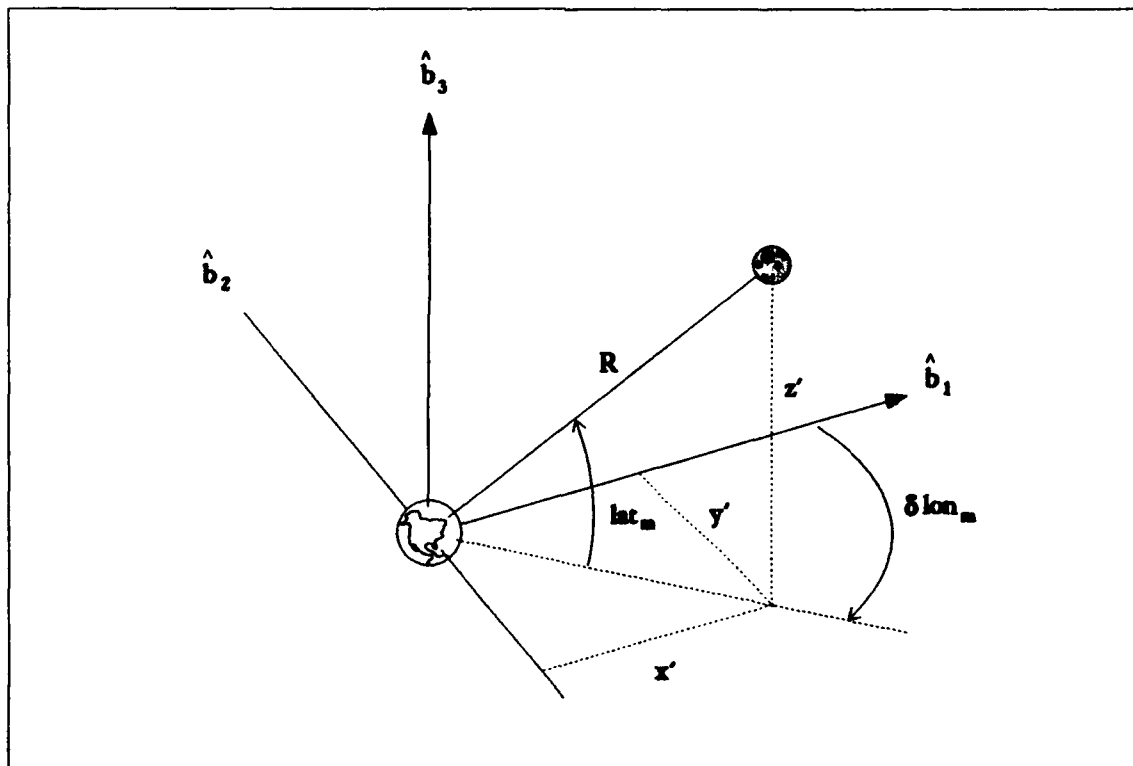


Figure 17. Rectangular ECR Coordinates from the Polar Coordinates.

The last coordinate transformation is a translation from the Earth Centered Rotating coordinate frame to the restricted three body (R3B) coordinate frame. This is accomplished simply by subtracting the distance between the two frames from the ECR position vector

$$\bar{r}_{R3B} = \bar{r}_{BCR} - \begin{bmatrix} (1-\mu) \\ 0 \\ 0 \end{bmatrix} \quad (73)$$

We now have the moon's position, for each of the five data points (times) near our chosen new moon, in the restricted three body problem coordinate system. A good approximation for the moon's position at the time of new moon, $\bar{r}(0)$, is derived from these five surrounding positions using the Lagrange Interpolation Formulas presented in the *Handbook of Mathematical Functions* (Abramowitz and Stegun, 1965:879). For our five point interpolation,

$$\begin{aligned} \bar{r}(0) = \bar{r}(u_0 + ah) \approx & \frac{(a^2 - 1)a(a - 2)}{24} \bar{r}(u_{-2}) - \frac{(a - 1)a(a^2 - 4)}{6} \bar{r}(u_{-1}) \\ & + \frac{(a^2 - 1)(a^2 - 4)}{4} \bar{r}(u_0) - \frac{(a + 1)a(a^2 - 4)}{6} \bar{r}(u_1) \\ & + \frac{(a^2 - 1)a(a + 2)}{24} \bar{r}(u_2) \end{aligned} \quad (74)$$

where h is the step size between each of the five ephemeris times, u_i are the five equally spaced ephemeris times, $\bar{r}(u_i)$ are the position vectors found from Eq (73), and a is the time difference between the third data point (u_0) and the time of new moon.

To get the initial velocity vector at the new moon time $\dot{\bar{r}}(0)$, we take the same five data points and use the derivative form of Lagrange's Formula (Abramowitz and Stegun, 1965:883)

$$\begin{aligned}\dot{\bar{r}}(0) = \dot{\bar{r}}(u_0 + ah) \approx \frac{1}{h} \left\{ \frac{2a^3 - 3a^2 - a + 1}{12} \bar{r}(u_{-2}) - \frac{4a^3 - 3a^2 - 8a + 4}{6} \bar{r}(u_{-1}) \right. \\ \left. + \frac{2a^3 - 5a}{2} \bar{r}(u_0) - \frac{4a^3 + 3a^2 - 8a - 4}{6} \bar{r}(u_1) \right. \\ \left. + \frac{2a^3 + 3a^2 - a - 1}{12} \bar{r}(u_2) \right\} \quad (75)\end{aligned}$$

Since $\bar{r}(t)$ and $\bar{q}(t)$ are the same thing, the initial inertial velocity vector, or generalized momenta vector, $\bar{p}(0)$ is calculated using Eqs (13)-(15) as

$$\bar{p}(0) = \begin{bmatrix} \dot{x} - y \\ \dot{y} + x \\ \dot{z} \end{bmatrix} \quad (76)$$

Finally, we have an initial state vector for the actual moon

$$\bar{x}(0) = \begin{pmatrix} \bar{q}(0) \\ \dots\dots\dots \\ \bar{p}(0) \end{pmatrix} \quad (77)$$

This state vector can now be used to develop the modal variables (§3.6) and determine if the real moon is in/near the linear regime of our periodic orbit.

3.7.2 Preliminary Results

It should not matter which new moon we select from the ephemerides, therefore we pick one at random. A real new moon occurred on 9 Feb 1967 at 1044 UT, so the five data times are spaced one day apart starting on 7 Feb at 0000 UT. The interpolation variables are shown below and the ephemerides are summarized in Appendix B.

$$h = 1.0 \text{ (days)} \quad a = \frac{644.0}{1440.0} \text{ (days)}$$

$$u_{-2} = 7 \text{ Feb } 0000 \text{ UT}$$

$$u_{-1} = 8 \text{ Feb } 0000 \text{ UT}$$

$$u_0 = 9 \text{ Feb } 0000 \text{ UT}$$

$$u_1 = 10 \text{ Feb } 0000 \text{ UT}$$

$$u_2 = 11 \text{ Feb } 0000 \text{ UT}$$

The interpolation method returns a restricted three body state vector for the new moon that looks like

$$\bar{x}(0) = \begin{bmatrix} -.997341 \\ -4.78964\text{E} - 7 \\ -2.29153\text{E} - 4 \\ \dots\dots\dots \\ 1.10990\text{E} - 3 \\ -.966821 \\ 3.79373\text{E} - 4 \end{bmatrix} \quad (77)$$

After doing the modal development, the modal variables are plotted and shown in Figures 18, 19, and 20. At best, we expect to see circles for the inclination and eccentricity modes and a straight line for the time/energy mode. At worst, we expect some higher frequency perturbations about the two circles and oscillating (but bounded) time and energy.

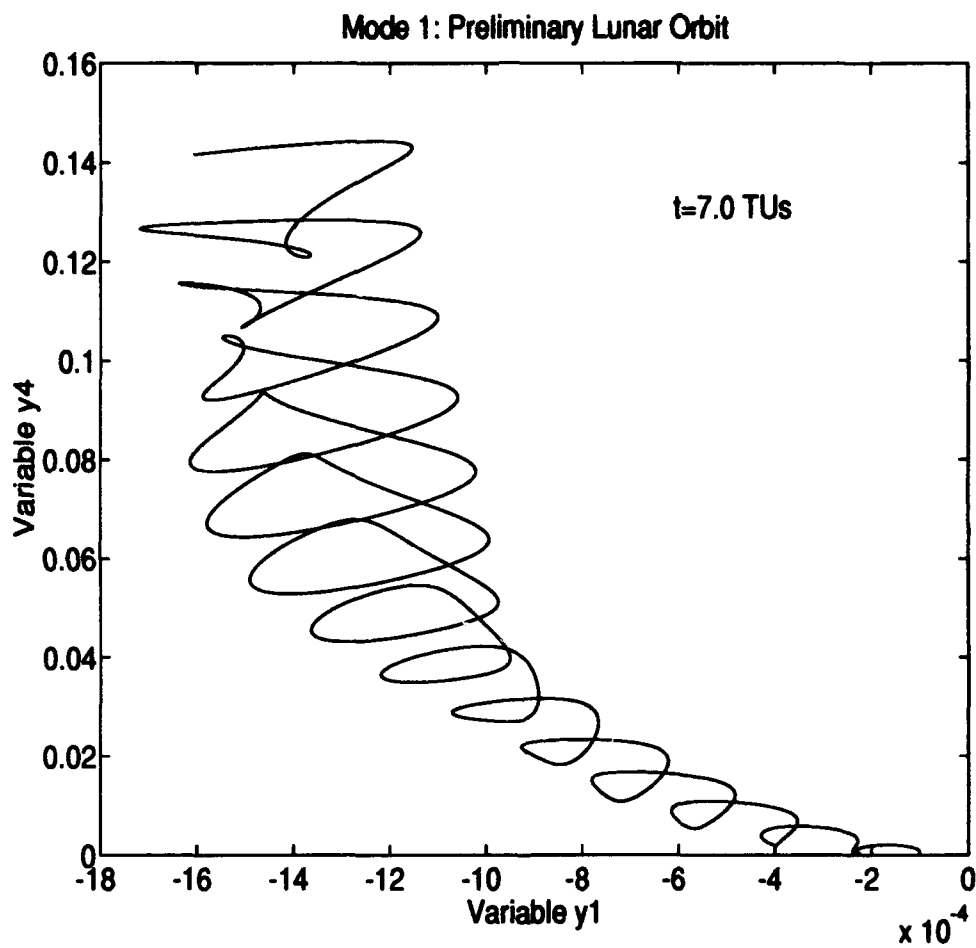


Figure 18. Time/Energy Mode using Preliminary Lunar Orbit Initial Conditions.

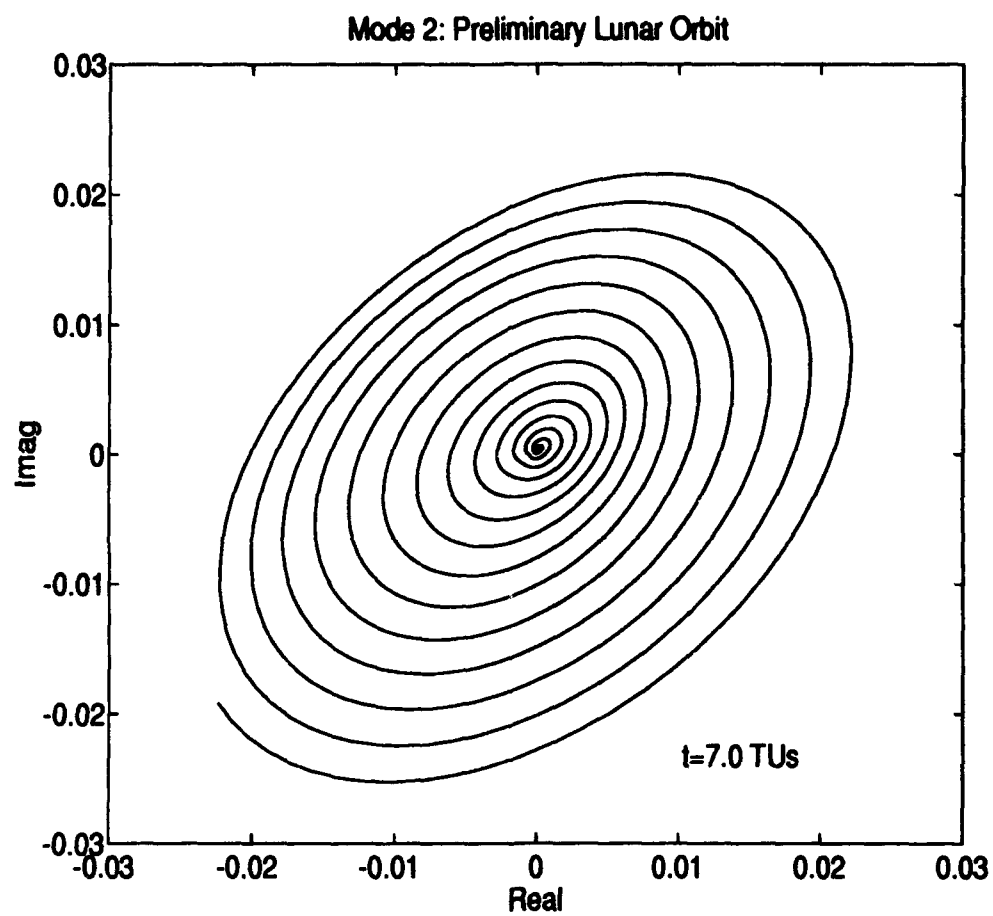


Figure 19. Inclination Mode using Preliminary Lunar Orbit Initial Conditions.

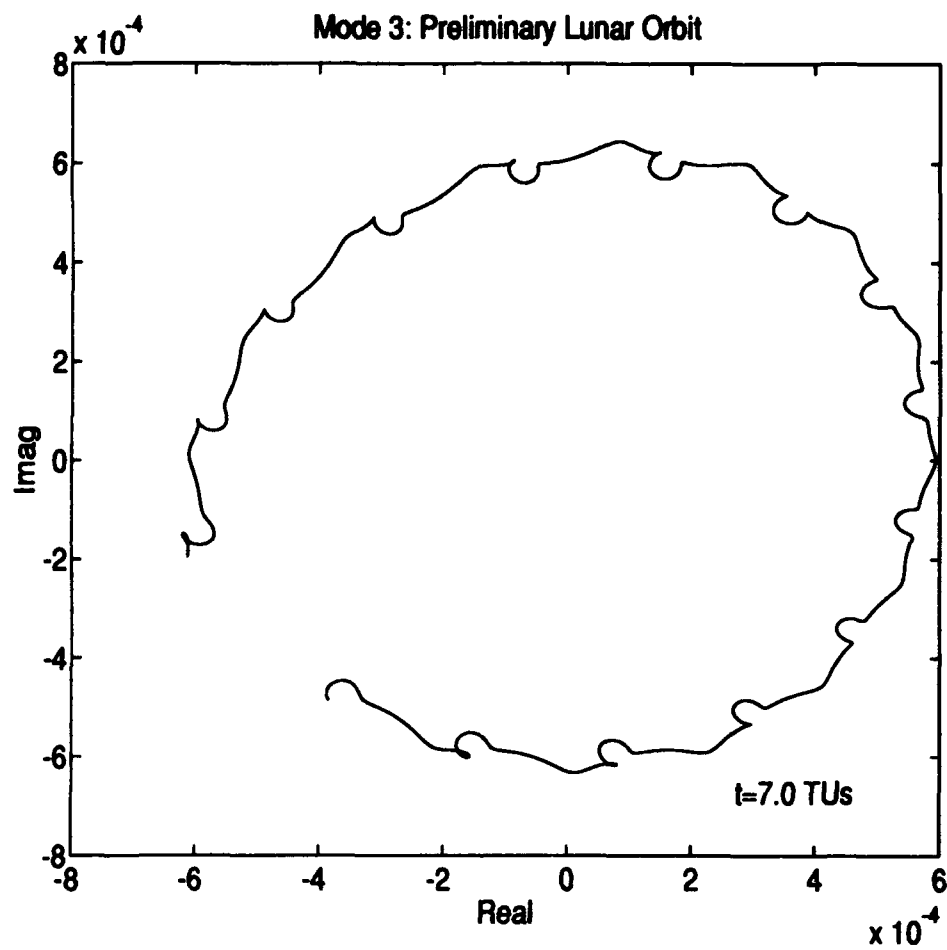


Figure 20. Eccentricity Mode using Preliminary Lunar Orbit Initial Conditions.

Obviously, there is a problem. While mode 3 looks somewhat close to a circle with perturbations, mode 2 spirals completely out of the periodic orbit's linear region. In addition, the energy (variable y_4) of the system seems to be going unbounded. To check these results, we choose another new moon from the ephemerides: 9 Feb 1986. These ephemerides, interpolation variables, and initial state vector are in Appendix C. The results from the Feb 86 data are very similar to the Feb 67 results.

The problem is two fold: 1) we are using initial conditions derived from real data for a particular month, but the period we are using is the average lunar period over history. The actual lunar period during Feb 67 is longer than the average value; 2) for the initial state vector

$$\bar{x}(0) = \begin{pmatrix} \bar{q}(0) \\ \dots\dots\dots \\ \bar{p}(0) \end{pmatrix}$$

we know that $\bar{q}(0)$ correctly matches the real world, but since $\bar{p}(0)$ is derived from the real world and our R3B model doesn't include everything the real world does, then $\bar{p}(0)$ does not provide our model with the initial conditions necessary to reproduce the moon's orbit.

To better illustrate the errors, reference Figure 21. This shows the X and Y components of the periodic orbit and the real orbit in physical, R3B coordinates. Both were integrated using the R3B model for the same amount of time. They are supposed to have the same period, but while the periodic orbit makes it back to the X-axis, the real orbit does not. Our dynamic model and average period are conflicting with what the ephemeris says the real orbit should be. Therefore the problem is this: given that $\bar{q}(t_0)$ is correct, find $\bar{p}(t_0)$ such that our R3B model will reproduce subsequent $\bar{q}(t_i)$'s that match real data.

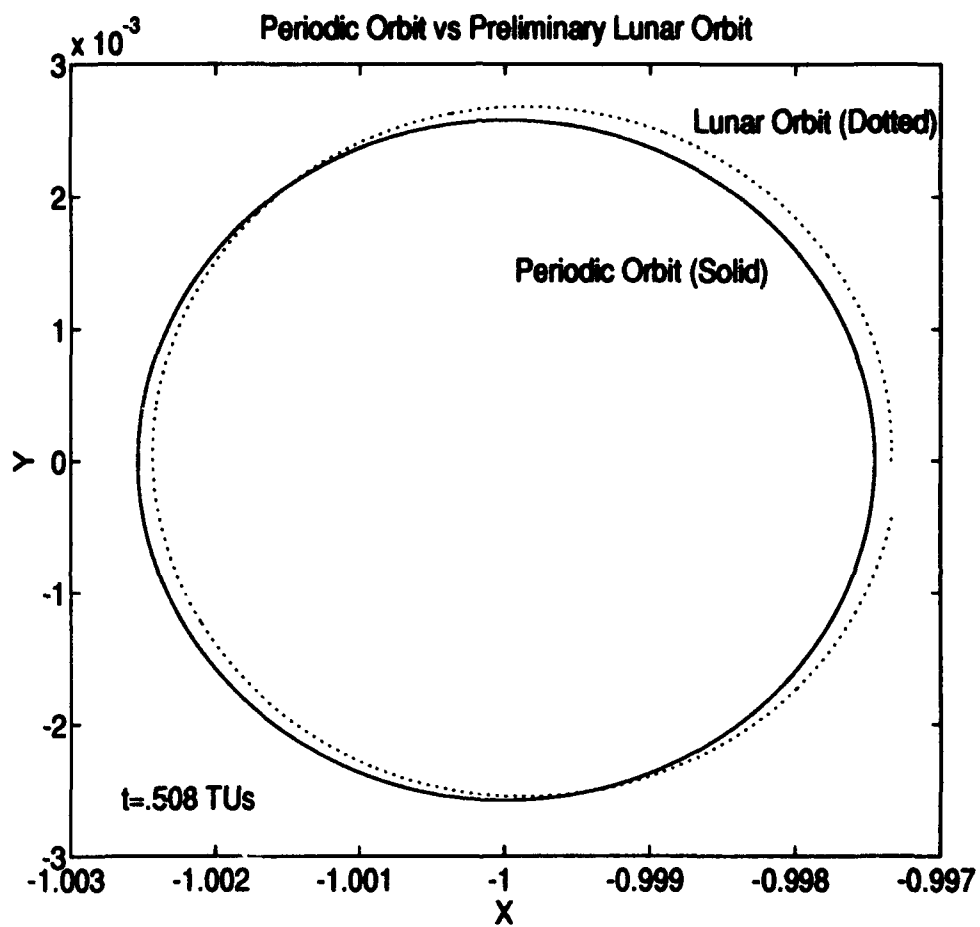


Figure 21. Periodic Orbit and Preliminary Lunar Orbit in Physical Space. X and Y components of the Restricted Three Body Problem.

3.7.3 Fitting the Initial Momenta to Our Dynamics Model

The solution to the problem above is to iteratively fit the initial momenta such that the integrated position matches the desired real position. The process is similar to finding the periodic orbit initial conditions (§3.2).

We start by picking some later time, t_1 , after the new moon and collecting more data. The ephemeris is converted with the same coordinate transformations explained in section 3.7.1 to get the position vector $\bar{r}_{eph}(t_1)$. The initial new moon state vector (Eq (77)) is integrated forward in time to t_1 so that the error in position at t_1 is calculated.

$$\bar{e}(t_1) = \underbrace{\bar{r}_{eph}(t_1)}_{\text{ephemeris}} - \underbrace{\bar{r}(t_1)}_{\text{integrated}} \quad (79)$$

Now Eq (27) is again recalled,

$$\delta \bar{x}(t_1) = \Phi(t_1, t_0) \delta \bar{x}(t_0)$$

$$\begin{pmatrix} \delta \bar{r}(t_1) \\ \delta \bar{p}(t_1) \end{pmatrix} = \begin{pmatrix} \Phi_{11} & \Phi_{12} \\ \Phi_{21} & \Phi_{22} \end{pmatrix} \begin{pmatrix} \delta \bar{r}(t_0) \\ \delta \bar{p}(t_0) \end{pmatrix} \quad (80)$$

so if we assume that the initial position is correct ($\delta \bar{r}(t_0) = 0$) and the differences in final momenta ($\delta \bar{p}(t_1)$) are unimportant, then we can isolate only the parts that concern us to get

$$\delta \bar{r}(t_1) = \Phi_{12} \delta \bar{p}(t_0) \quad (81)$$

$$-\bar{e}(t_1) = \Phi_{12} \delta \bar{p}(t_0) \quad (82)$$

Solving for $\delta \bar{p}(t_0)$ yields the correction to the initial momenta vector so that

$$\bar{p}(t_0)_{new} = \bar{p}(t_0)_{old} + \delta \bar{p}(t_0) \quad (83)$$

This new initial momenta vector is substituted back into the initial state vector and the cycle is repeated until the error meets some tolerance (we used 10^{-10}). When the error is small

enough, we have a set of initial conditions that, when integrated forward with our R3B dynamics model, echo the actual lunar ephemeris for time t_1 . We then pick a new value for t_1 , and use those initial conditions as a new first guess. The process is continued until a large enough t_1 is found such that the average period of the real orbit matches the period of the periodic orbit.

The end product here is an initial state vector that will yield the exact modal representation of the lunar orbit.

3.8 Perturbation Theory

In the last section, we developed the *exact* modal representation of the moon's orbit. Here, the goal is to develop an *expanded* modal solution. That is, we want the equations of motion for the modal variables based on the perturbation expansion of the new modal Hamiltonian.

We start with the original Hamiltonian, $\mathcal{H}(\bar{x})$, and expand it in a Taylor's series about the periodic orbit (i.e. $\bar{x} = \bar{x}_p$ or $\delta\bar{x} = 0$).

$$\mathcal{H}(\bar{x}) = \mathcal{H}_0 + \mathcal{H}_1 + \mathcal{H}_2 + \mathcal{H}_3 + \mathcal{H}_4 + \dots$$

$$\mathcal{H}_0 = \mathcal{H}(\bar{x}_p)$$

$$\mathcal{H}_1 = \sum_{\mu=1}^6 \left. \frac{\partial \mathcal{H}}{\partial x_{\mu}} \right|_{\delta\bar{x}=0} \delta x_{\mu}$$

$$\mathcal{H}_2 = \frac{1}{2!} \sum_{\mu=1}^6 \sum_{\nu=1}^6 \left. \frac{\partial^2 \mathcal{H}}{\partial x_{\mu} \partial x_{\nu}} \right|_{\delta\bar{x}=0} \delta x_{\mu} \delta x_{\nu}$$

$$\mathcal{H}_3 = \frac{1}{3!} \sum_{\mu=1}^6 \sum_{\nu=1}^6 \sum_{\lambda=1}^6 \left. \frac{\partial^3 \mathcal{H}}{\partial x_{\mu} \partial x_{\nu} \partial x_{\lambda}} \right|_{\delta\bar{x}=0} \delta x_{\mu} \delta x_{\nu} \delta x_{\lambda}$$

⋮

(84)

The tensor notation for Eq (84) is

$$\mathcal{H}(\bar{x}) = \mathcal{H}_0 + \mathcal{H}_{1,\mu} \delta x_{\mu} + \frac{1}{2!} \mathcal{H}_{2,\mu\nu} \delta x_{\mu} \delta x_{\nu} + \frac{1}{3!} \mathcal{H}_{3,\mu\nu\lambda} \delta x_{\mu} \delta x_{\nu} \delta x_{\lambda} + \dots \quad (85)$$

The first term, \mathcal{H}_0 , is a scalar constant because it is the Hamiltonian for the periodic orbit.

For simplicity, we choose the scalar constant to be zero. "The second, or linear term is identically zero, because it describes the motion of the periodic trajectory with respect to itself.

The third, or quadratic term is the Floquet problem, and becomes a constant coefficient, linear system in the new variables" (Ross, 1991:31). Therefore, the expanded Hamiltonian now looks like

$$\mathcal{H}(\bar{x}) = \frac{1}{2!} \mathcal{H}_{2,\mu\nu} \delta x_\mu \delta x_\nu + \frac{1}{3!} \mathcal{H}_{3,\mu\nu\lambda} \delta x_\mu \delta x_\nu \delta x_\lambda + \frac{1}{4!} \mathcal{H}_{4,\mu\nu\lambda\sigma} \delta x_\mu \delta x_\nu \delta x_\lambda \delta x_\sigma + \dots \quad (86)$$

By writing the transformation to modal variables $\delta \bar{x} = E \bar{y}$ in tensor notation $\delta x_i = e_{ij} y_j$, we can canonically transform Eq (86) to the new expanded Hamiltonian in modal variables, $\mathcal{H}(\bar{y})$.

$$\mathcal{H}(\bar{y}) = \frac{1}{2!} \mathcal{K}_{2,ij} y_i y_j + \frac{1}{3!} \mathcal{K}_{3,ijk} y_i y_j y_k + \frac{1}{4!} \mathcal{K}_{4,ijkl} y_i y_j y_k y_l + \dots \quad (87)$$

where

$$\mathcal{K}_{2,ij} = \mathcal{H}_{2,\mu\nu} e_{\mu i} e_{\nu j} \quad (88)$$

$$\mathcal{K}_{3,ijk} = \mathcal{H}_{3,\mu\nu\lambda} e_{\mu i} e_{\nu j} e_{\lambda k} \quad (89)$$

$$\mathcal{K}_{4,ijkl} = \mathcal{H}_{4,\mu\nu\lambda\sigma} e_{\mu i} e_{\nu j} e_{\lambda k} e_{\sigma l} \quad (90)$$

The $\mathcal{K}_{2,ij}$ term is the constant, symmetric matrix S introduced earlier (§3.3). The $\mathcal{K}_{3,ijk}$, $\mathcal{K}_{4,ijkl}$, and higher terms are periodic tensors since the partials tensors (\mathcal{H} terms) and the E matrix are both periodic with the same period as our periodic orbit. We get the partials tensors as well as the elements of the E matrix from the Fourier coefficients of $\bar{x}_p(t)$ and $E(t)$ just as before.

As mentioned in section 3.4, making $\bar{y}(t) = E^{-1}(t) \delta \bar{x}(t)$ a canonical transformation ensures that the new modal Hamiltonian $\mathcal{H}(\bar{y})$ follows Hamilton's equations. This is useful, because we want *modal equations of motion* and we get them from Hamilton's equations:

$$\dot{\bar{y}} = Z \frac{\partial \mathcal{X}(\bar{y})}{\partial \bar{y}} \quad (91)$$

Again, using tensor notation, we get

$$\dot{y}_i = \left(Z \nabla(\mathcal{X})_y \right)_i = Z \mathcal{X}_{2,ij} y_j + \frac{1}{2!} Z \left(\mathcal{X}_{3,ijk} y_j y_k \right) + \frac{1}{3!} Z \left(\mathcal{X}_{4,ijkl} y_j y_k y_l \right) + \dots \quad (92)$$

The first term is the constant coefficient, linear system we established with Eq (48), where $Z \mathcal{X}_{2,ij} = Z S = J$. By itself, $\dot{y}_i = J_{ij} y_j$ should create modal plots that are perfect circles, saddles, and straight lines for the respective modes. The second, third, and subsequent terms represent the perturbations off of the linear system.

We now have equations of motion in terms of the modal variables, with initial conditions derived by canonically transforming the initial state vector from physical variables. The modal plots from this expansion solution should compare closely with those from the exact solution discussed in the last section.

Specifically in our case, when the expansion only includes the \mathcal{X}_2 term, we should get perfect circles for the inclination and eccentricity modes and a straight line for the time/energy mode. As each of the additional perturbation terms are included in the expansion, the modal plots should agree more and more closely. If all of the most significant terms are included, the two modal representations should match well. As Fourier series computations get extremely cumbersome beyond the third term, we choose to limit our expansion to \mathcal{X}_4 .

IV. Software

To do this study, several FORTRAN and MATLAB™ computer codes were used. This chapter discusses the specific software that was developed to accomplish each of the corresponding sections of Chapter Three. Although the software codes are not presented in this document, they can be reproduced from the information in Chapter Three or obtained from the author or Dr. Wiesel. Unless otherwise stated, each code was written in FORTRAN 77.

4.1 Periodic Orbit

The program PERIOD takes our initial conditions guess from section 3.2 (Eq (37)) and, using a predictor/corrector algorithm called HAMING, iterates toward a nearby set of initial conditions that when integrated for one period, creates a periodic orbit. PERIOD is set up specifically to handle symmetric periodic orbits in the restricted three body problem. The iteration process was discussed in more detail in section 3.2.2. After finding the periodic orbit initial conditions, PERIOD calculates the monodromy matrix, eigenvalues, eigenvectors (F matrix), and Poincaré exponents (J matrix) as described in section 3.3.

4.2 Symplectic Normalization

Before doing the symplectic normalization, the RPEXVEC code is needed to determine the restricted problem extended (or generalized) eigenvector for those systems, like ours, with degenerate modes. RPEXVEC uses hardwired values from selected rows of the monodromy matrix (Φ) and the conjugate eigenvector (\bar{f}_1) to solve Eq (67) for the extended eigenvector \bar{f}_4' using a linear equations solver. The eigenvector matrix F is modified accordingly and fed into program SYMNRM.

SYMNRM does the actual symplectic normalization of F to E by calculating the diagonal entries of the D matrix (Eq (63)). The output of SYMNRM is the initial E matrix.

4.3 Modal Variable Development

The periodic orbit initial conditions, the J matrix, and the initial E matrix are all inputs to the MODEDV program. MODEDV integrates the periodic orbit and E matrix forward in time to one period, saving values of each at evenly spaced intervals. Using the harmonic analysis subroutine CMPFOR (based on the algorithm of Brouwer and Clemence (1961:108-113)), we then get a set of complex exponential Fourier coefficients for both the periodic orbit state vector and E (§ 3.6).

The Fourier coefficients are loaded into the program TRAJ, as is the initial condition state vector of some near-periodic trajectory. TRAJ integrates the near-periodic trajectory in discrete steps. At each step, TRAJ calls the subroutine MODEVR which sums the Fourier coefficients of the periodic orbit and E , and calculates the modal vector using Eq (69). The result is a series of modal vectors evenly spaced throughout the integration time. These modal vectors are then easily plotted as discussed in section 3.6.

4.4 Real Moon Initial Conditions from Data (Exact Solution)

A MATLAB™ code called FEB67.m is used to calculate the real moon's initial conditions from February 1967 data (an identical code called FEB86.m was also created for 1986 data). The sun/moon information is loaded for five evenly spaced times around the new moon, transformed into the Earth Centered Rotating frame, and finally translated to the restricted three body frame. FEB67.m then interpolates to get the moon's position and velocity vector's as shown in section 3.7.1. After doing one last transformation of the velocity vector to the inertial velocity vector, FEB67.m returns an initial condition state vector for the actual moon. This initial condition state vector is nominally loaded into program TRAJ as the near-periodic trajectory. However, it was shown in section 3.7.2 that the initial momenta needs to be fitted to our dynamics model.

Program FITICS takes the initial new moon state vector (output from FEB67.m), and iterates toward an initial momenta vector such that the integrated position matches the position listed in the ephemerides at some time after new moon. The process is similar to that used for program PERIOD and the details are shown in section 3.7.3. The output of FITICS is the new initial condition state vector that is entered into TRAJ as the near-periodic trajectory.

4.5 Expanded Modal Solution

There are three main programs used to create the modal expansion plots: K3DEV, K4DEV, and YTRAJ. K3DEV develops the third order periodic tensor ($\mathcal{X}_{3,ijk}$) of the expanded Hamiltonian in modal variables. At each evenly spaced time, K3DEV reads in and sums the Fourier coefficients for the periodic orbit state and E . Then, the third order partial tensor of the original Hamiltonian ($\mathcal{H}_{3,\mu\nu\lambda}$) is retrieved from subroutine ORDER3. Using the summation convention shown in section 3.8, we get the third order tensor ($\mathcal{X}_{3,ijk}$) at evenly spaced times throughout the period. Again using the harmonic analysis subroutine CMPFOR, we get a series of Fourier coefficients for $\mathcal{X}_{3,ijk}$.

K4DEV does the same thing as K3DEV except that it uses subroutine ORDER4 and finds the *fourth* order periodic tensor, $\mathcal{X}_{4,ijkl}$, of the expanded Hamiltonian in modal variables.

Program YTRAJ is the counterpart of TRAJ. Instead of integrating the orbit in physical variables and transforming to modal variables at each step, YTRAJ integrates the modal variables directly. The initial state vector is transformed from physical variables to modal variables, and the $\mathcal{X}_3 / \mathcal{X}_4$ Fourier coefficients are read in. At each time step, the \mathcal{X}_3 and \mathcal{X}_4 Fourier coefficients are summed and the modal variables are integrated by Eq (92). The result of YTRAJ is a series of modal vectors that, when plotted over time, should match the plotted results of TRAJ.

V. Results and Discussion

5.1 Exact Modal Results

In section 3.7.1, we find an initial state vector in physical variables for the real moon, however, the initial momenta needs to be fitted such that the model integrations match the real data at a future time (section 3.7.3). To do the fitting, values of t_1 are selected starting with two weeks after the new moon. Next, one month is tried, then six months, and finally one year after the new moon. The result is a well approximated initial condition state vector in physical variables for the moon. This initial lunar state vector is the near-periodic orbit that is integrated and transformed to modal variables using the TRAJ program. The modes produced are what we call the exact modal representation.

As stated earlier, the first result of interest is whether the lunar orbit is in or near the linear region of the periodic orbit. The modal plots of the exact modal representation are shown in Figures 22, 23, and 24. Figure 22 is a plot of the time/energy mode (mode 1). The epoch time displacement (variable y_1) is shown oscillating back and forth, which basically represents *in-track* fluctuations of the moon's orbit about the original periodic orbit. The system energy (variable y_4) is also shown oscillating, however it is bounded. Of the three modes, mode 1 has the least stringent requirements for acceptable behavior. As a general rule, according to Dr. Wiesel, the time/energy mode is considered to be behaving reasonably as long as the energy stays bounded. As you can see, it does stay bounded.

The next plot is the inclination mode, or mode 2, shown in Figure 23. We are looking for something close to a circle, and that is basically what we get. The plot shows higher frequency oscillations about a generally circular motion. These higher frequency loops characterize the perturbations to the linear Floquet periodic orbit. In fact, the number of higher frequency loops in the pattern (three) corresponds to the order of dominant terms in the Fourier series. Given the relative size of the oscillations, we can conclude that this mode is not necessarily in the linear regime, but it is definitely close.

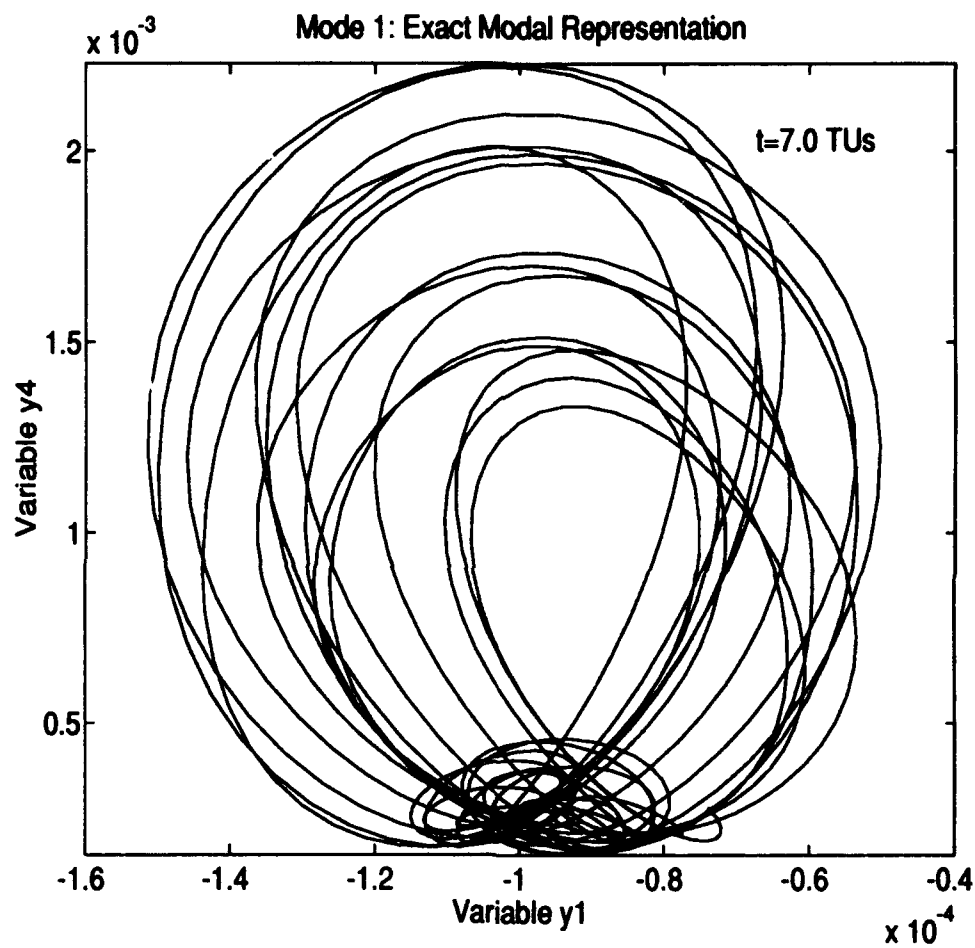


Figure 22. Exact Modal Representation of the Time/Energy Mode using Fitted Initial Conditions.

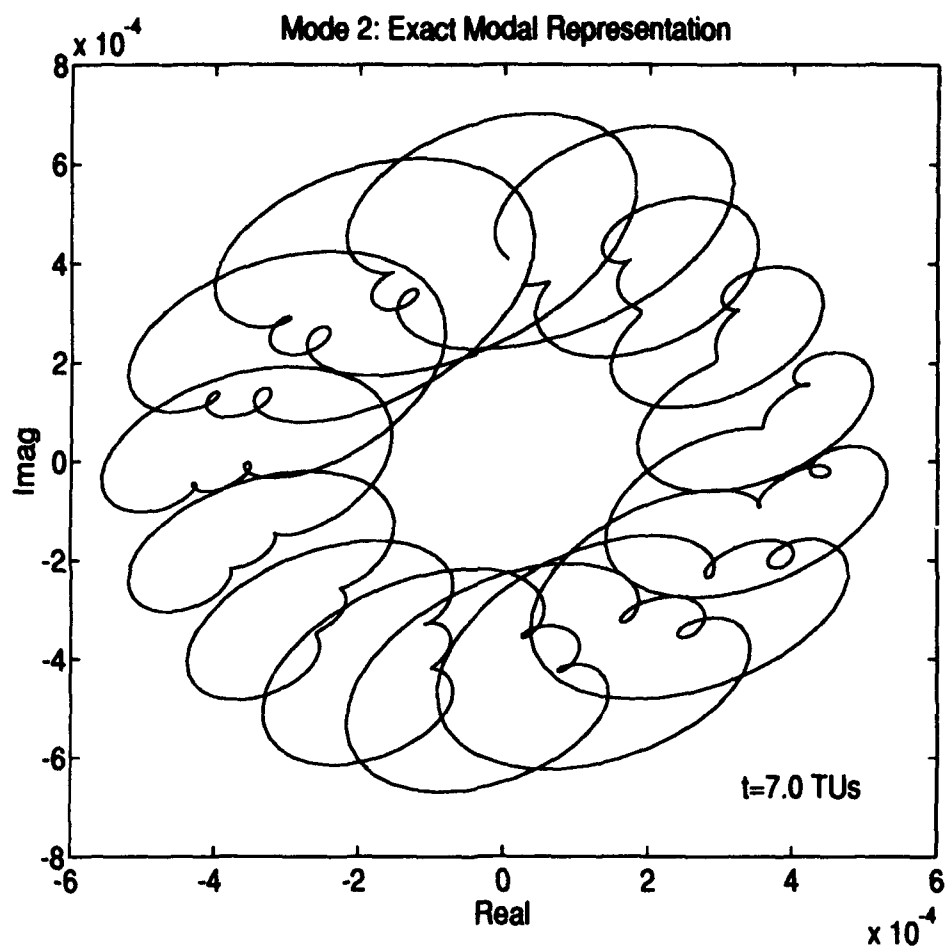


Figure 23. Exact Modal Representation of the Inclination Mode using Fitted Initial Conditions.

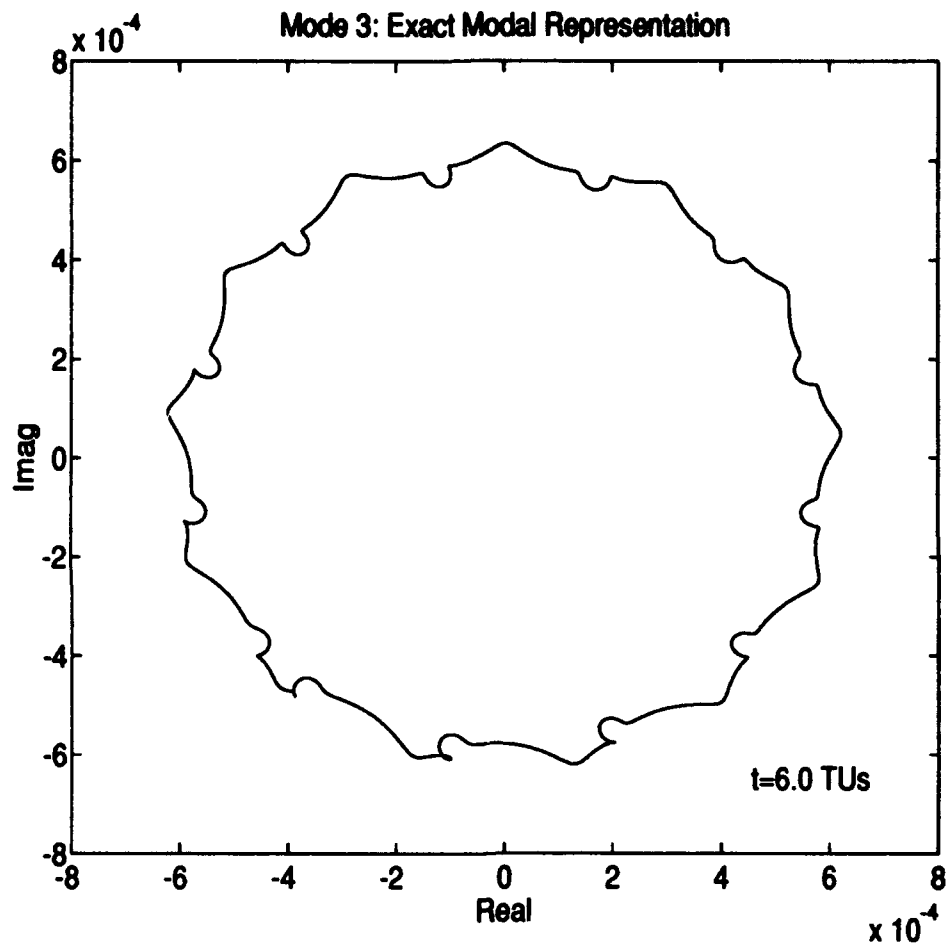


Figure 24. Exact Modal Representation of the Eccentricity Mode using Fitted Initial Conditions.

Figure 24 shows the plot for mode 3, the eccentricity mode. As with mode 2, we expect to see a circle and again, the plot shows a circle with higher frequency oscillations. In this case, however, the eccentricity mode's motion is definitely closer to a perfect circle. Therefore, mode 3 is close to the linear regime, but not quite in it.

Looking at all three modal plots, it is concluded that the moon's real orbit is not in the linear region of the periodic orbit, but it *is* close enough that we can see the reference linear behavior about which the higher frequency oscillations are being perturbed. The next step is to proceed with the rest of the analysis and compare these exact modal plots with the expanded modal plots. They should match closely.

5.2 Expanded Modal Results

In this section we present the modal plots that are derived from the modal equations of motion based on the perturbation expansion of the new modal Hamiltonian (Eq (92)). These plots are the results of program YTRAJ, and we call them the expanded modal representation. They are compared with the exact modal representation results from the last section. The two modal representations should match closely if we include enough perturbation expansion terms. The comparison accomplishes three things:

1. It provides redundancy of the exact modal plots to satisfy ourselves that the technique was properly applied.
2. It verifies that we have successfully transformed the Hamiltonian itself to modal coordinates.
3. It determines if the perturbations are mostly (or entirely) derived from only the \mathcal{K} -terms that we choose to include in the expansion.

We first run the YTRAJ program only considering the first term (\mathcal{K}_2) of the expanded representation. The expanded modal plots are overlaid with the exact modal plots

and the results are shown in Figures 25, 26, and 27. As discussed in section 3.8, the \mathcal{X}_2 expansion term by itself represents a constant coefficient, linear system. It is the Floquet portion of the expansion and it exhibits perfect linear behavior. For modes 2 and 3 (Figures 26 and 27), we get a perfect circle that overlays nicely with the exact modal plot to show the path about which they are perturbed. Mode 1 (Figure 27) is a perfectly straight line as expected, where energy is fixed. If the lunar orbit was in the linear regime of the periodic orbit, the \mathcal{X}_2 term would essentially be the only term in the expansion necessary to match the two representations. But since the moon is definitely outside the linear region, we need to include the perturbation terms. As we include more term in the expansion, we should start perturbing off of the perfect circles/line, and start matching the exact modal plots more closely.

The YTRAJ program is run again, but this time the \mathcal{X}_3 term is added to the expansion. These modal plots are overlaid with the exact modal plots and shown in Figures 28, 29, and 30. The results are unreasonable in that the expanded plots initially follow the exact solution plots, but then spiral off toward infinity. For example, Figure 29 shows that mode 2 stays with the first high frequency perturbation loop for a while, but then quickly spirals away. The best thing to do is to continue adding perturbation terms to the expansion.

Now YTRAJ is run with all terms in the expansion out to the \mathcal{X}_4 term. The modal plots are again overlaid with the exact solution and presented in Figures 31, 32, and 33. They show definite improvement over the previous two sets of modal plots. The expansion modes stay with the exact modes a lot longer this time, but they still eventually spiral off toward infinity. Again using mode 2 (Figure 32) as an example, the behavior matches quite well for the first three or four perturbation loops before it spirals away. The conclusion again, is that more perturbation terms need to be considered in the expansion. However, instead of dealing with a computational nightmare, there is an attractive alternative.

It is our contention that the plots would match if we added enough terms to the expansion, but because the real moon is not in the linear region of the periodic orbit it takes a great number of the expansion terms to get a perfect match. Consider that \mathcal{X}_{ijk} is a $6 \times 6 \times 6$

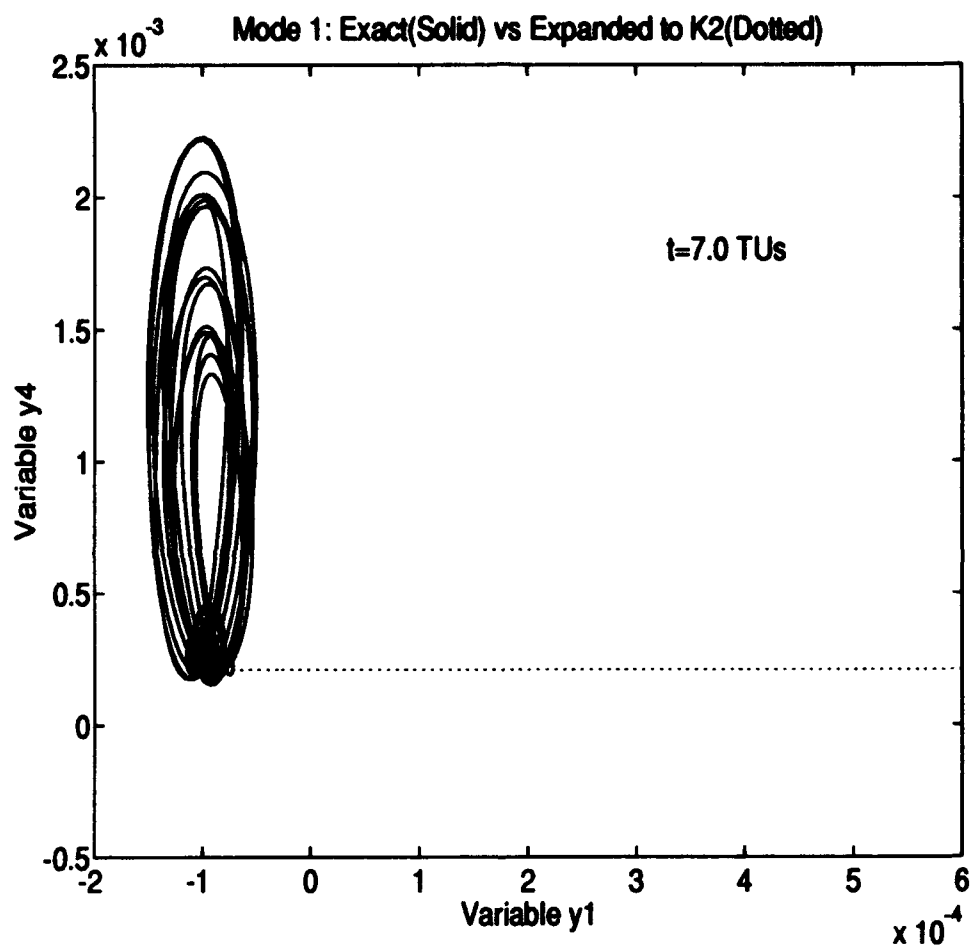


Figure 25. Exact vs Expanded Modal Solution (K2 Only). Time/Energy Mode.

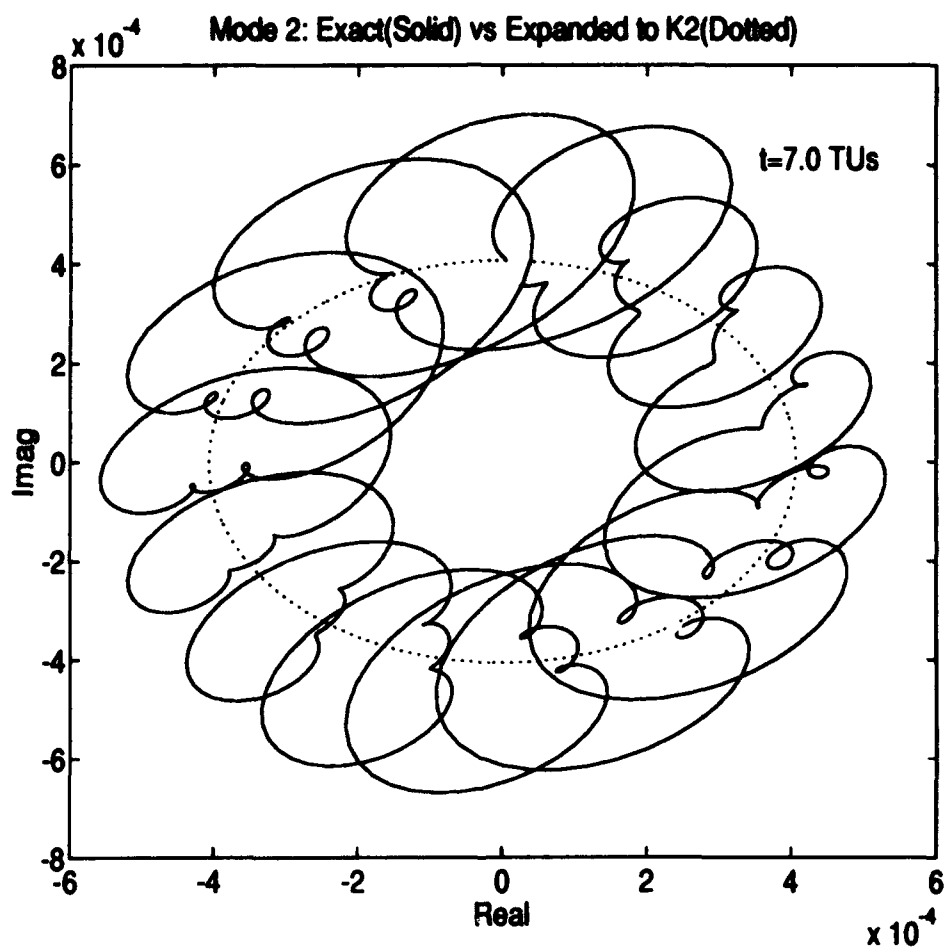


Figure 26. Exact vs Expanded Modal Solution (K2 Only). Inclination Mode.

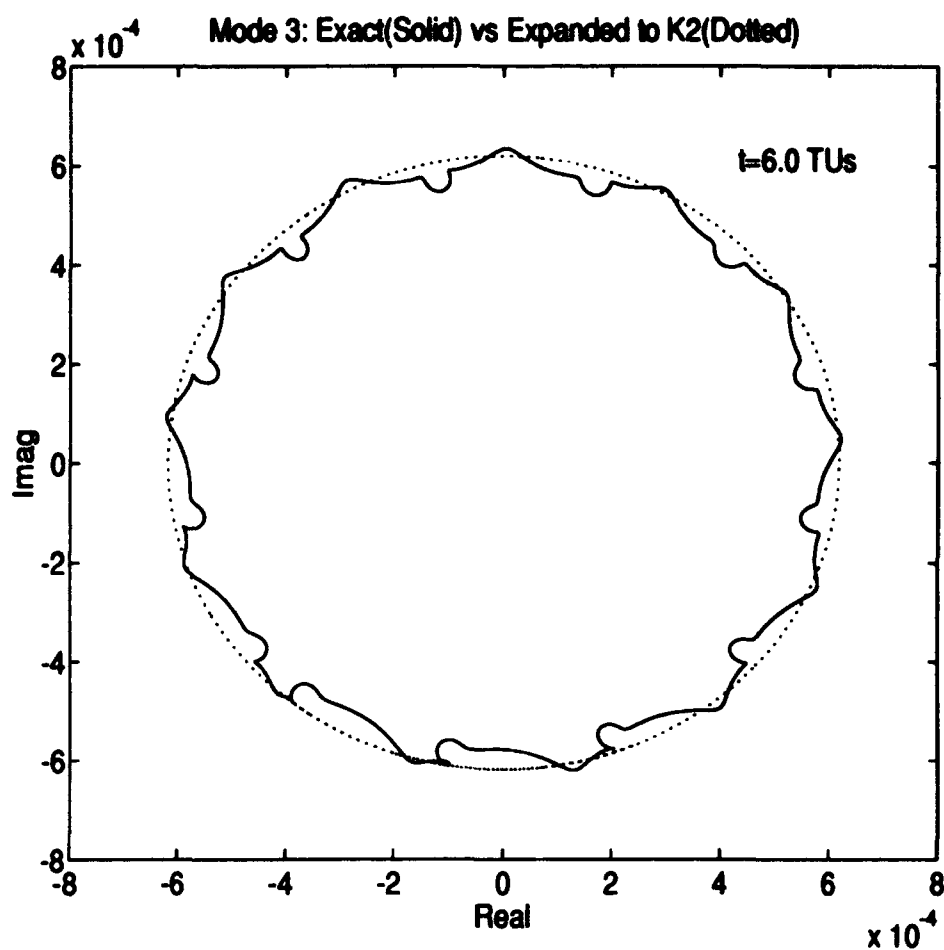


Figure 27. Exact vs Expanded Modal Solution (K2 Only). Eccentricity Mode.

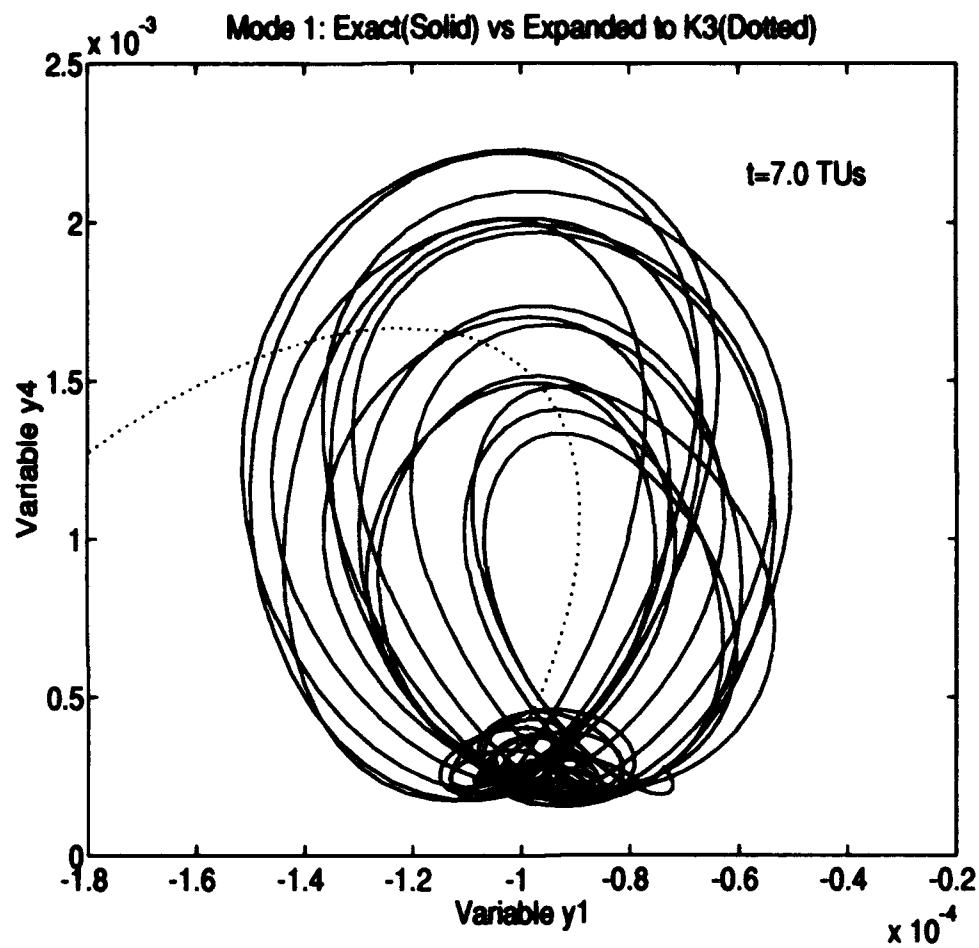


Figure 28. Exact vs Expanded Modal Solution (K2 & K3 Only). Time/Energy Mode.

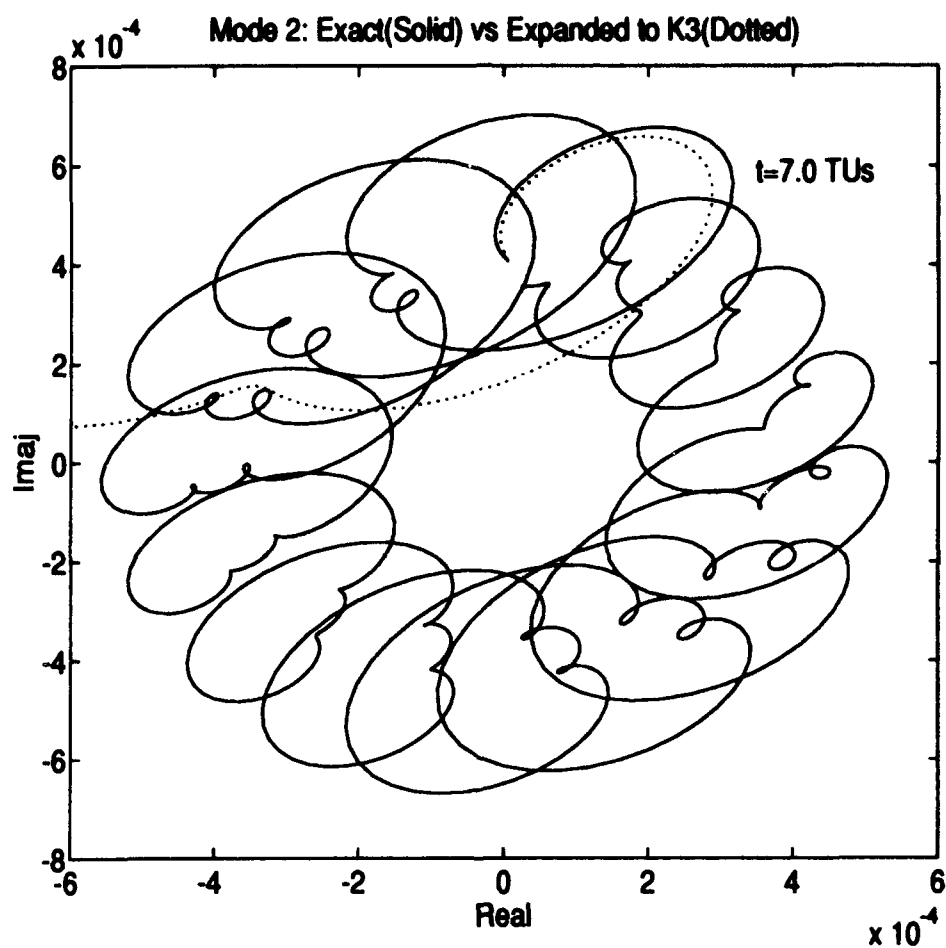


Figure 29. Exact vs Expanded Modal Solution (K2 & K3 Only). Inclination Mode.

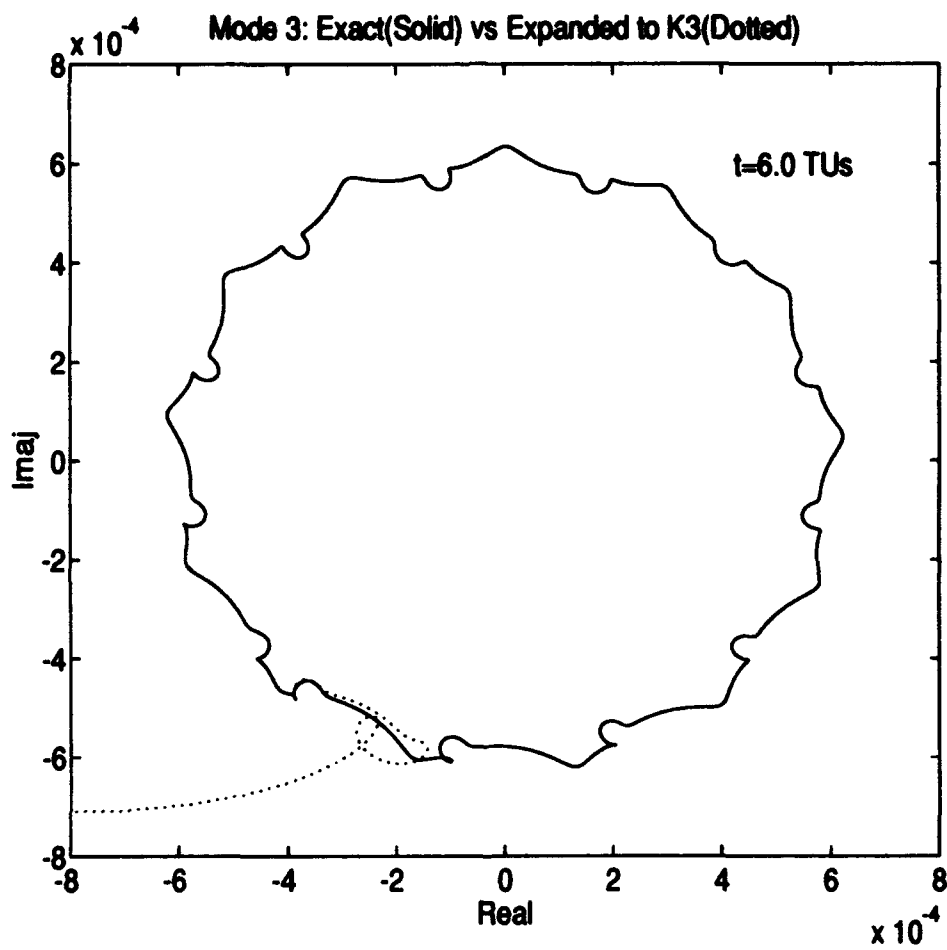


Figure 30. Exact vs Expanded Modal Solution (K2 & K3 Only). Eccentricity Mode.

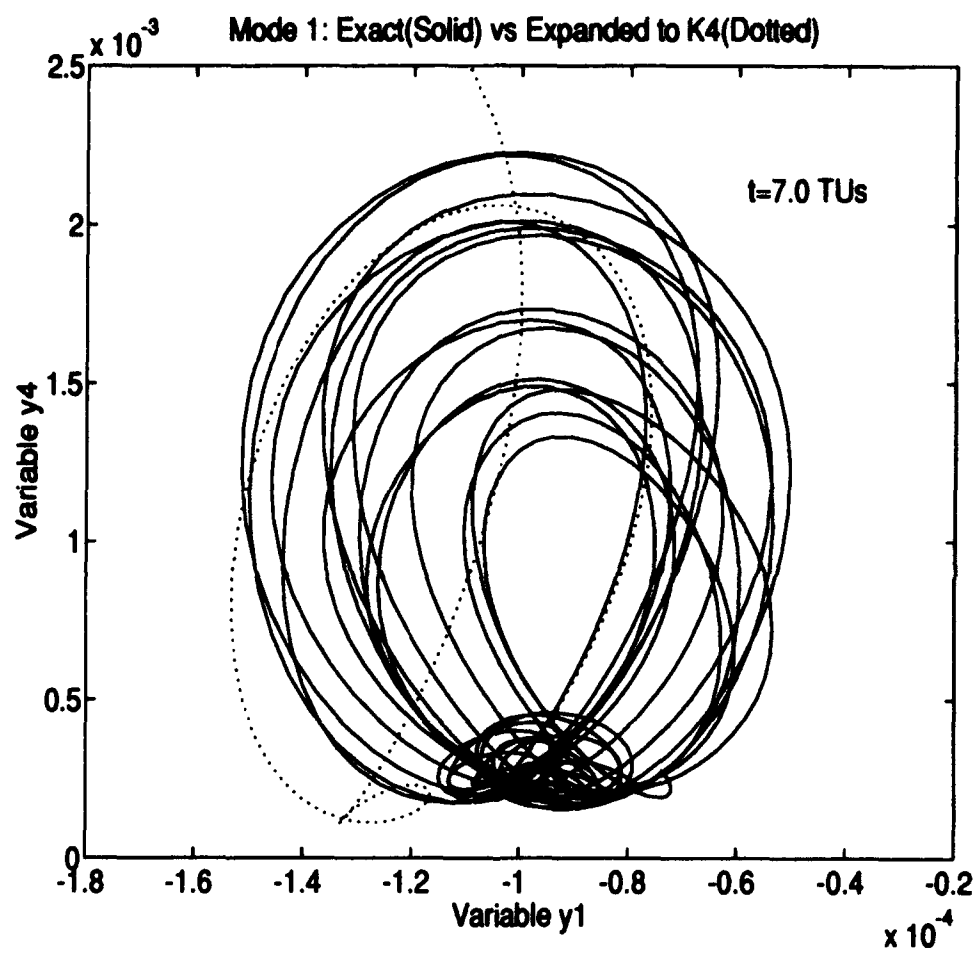


Figure 31. Exact vs Expanded Modal Solution (K2, K3 & K4). Time/Energy Mode.

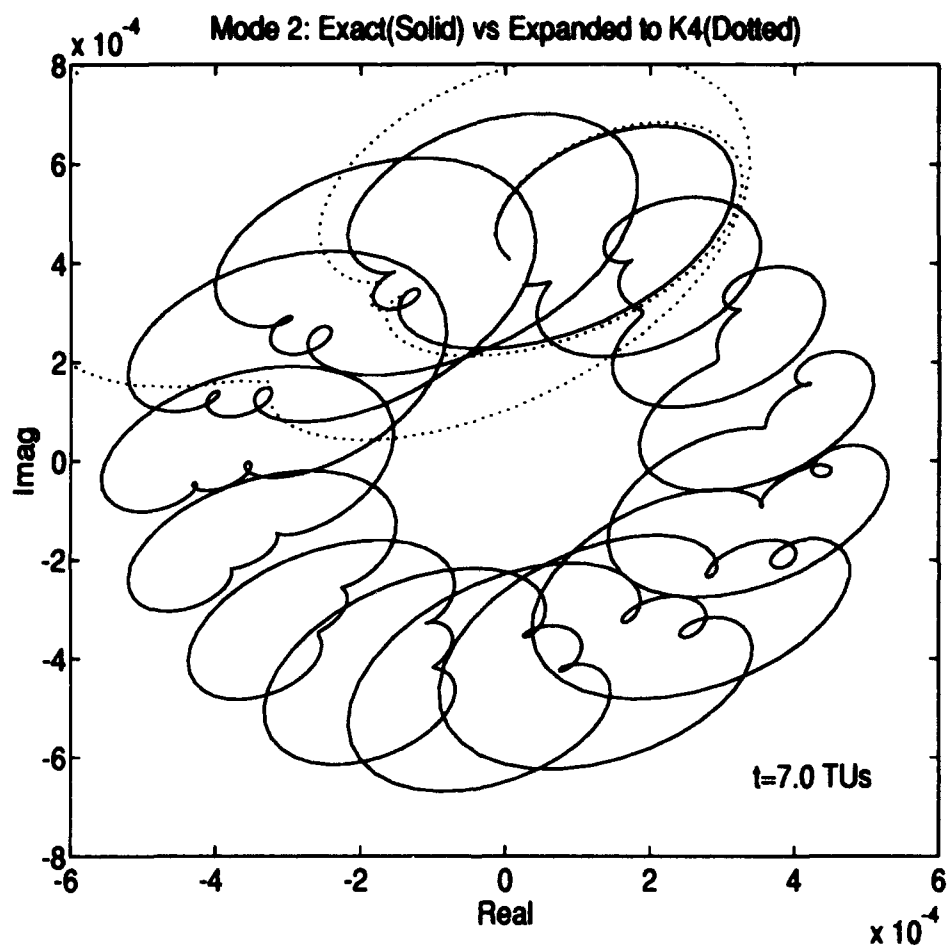


Figure 32. Exact vs Expanded Modal Solution (K2, K3 & K4). Inclination Mode.

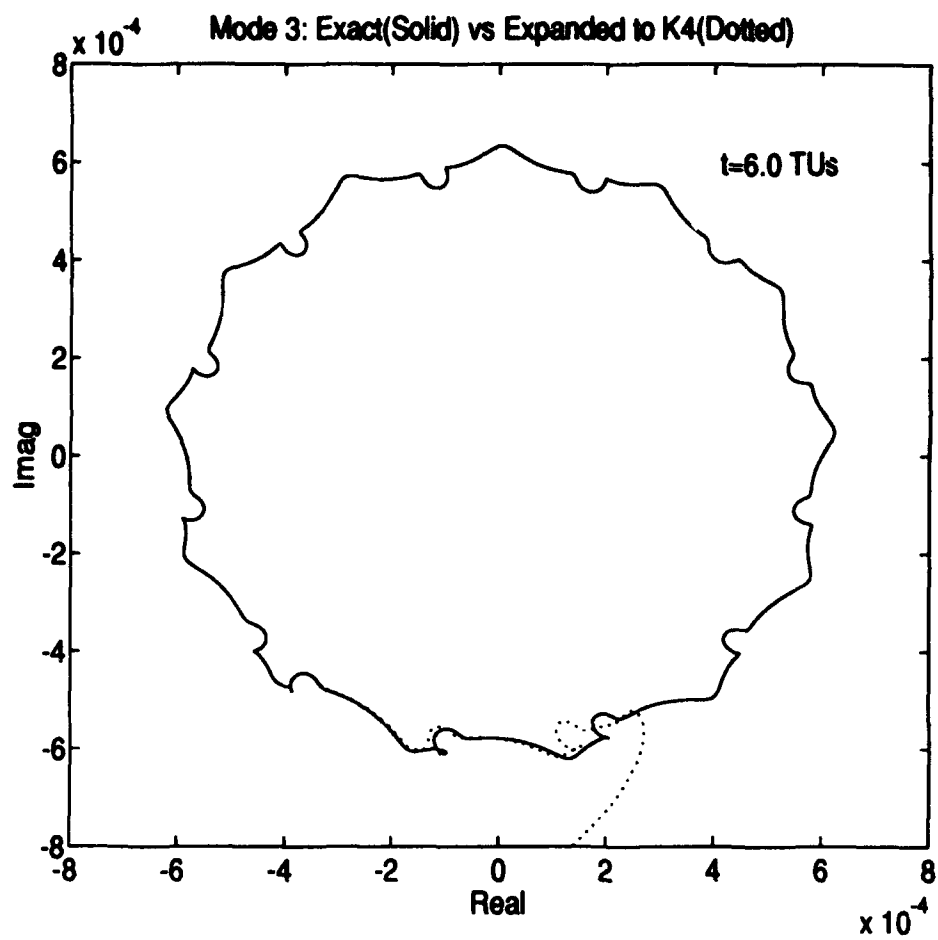


Figure 33. Exact vs Expanded Modal Solution (K2, K3 & K4). Eccentricity Mode.

tensor, $\mathcal{K}_{4,ijkl}$ is a $6 \times 6 \times 6 \times 6$ tensor, and that each element of those tensors has 41 Fourier coefficients. The computational requirements of the $6 \times 6 \times 6 \times 6 \times 6 \times 41$ (or higher) array needed to facilitate the \mathcal{K}_5 (or higher) term would obviously be great.

Rather than deal with the laborious task of including the \mathcal{K}_5 , \mathcal{K}_6 , etc. terms to get the modal plots to match, we created a fictitious moon that exhibits the same basic dynamics of the real moon but is much closer to the linear regime of the periodic orbit. To get this fictitious moon, we decrease the amplitude of the real moon's modes by taking the initial conditions in modal variables and dividing by an arbitrary constant (we use 10.0). The initial conditions in physical variables are calculated from Eq (46) as

$$\delta \bar{x}(0) = F(0) \bar{y}(0) \quad (93)$$

and loaded into program TRAJ. The result is a set of exact modal plots for the fictitious moon. Meanwhile, the initial conditions in modal variables are loaded into program YTRAJ, where the only expansion terms included are \mathcal{K}_2 , \mathcal{K}_3 , and \mathcal{K}_4 . The result is a set of expanded modal plots for the fictitious moon. These new modal plots are compared and shown in Figures 34, 35, and 36.

Obviously, the fictitious moon is much closer than the real moon to the linear region of the periodic orbit. In fact, mode 3 (Figure 36) is basically a perfect circle. Since we are so much closer to the linear regime, we expect that less expansion terms are required to get the exact and expanded results to match. That is definitely the case here. The exact and expanded modes match very closely. Mode 1 (Figure 34) breaks down the earliest of the three modes, but even so, the form compares close enough to make the point and it shows behavior that is much closer to pure time drift with bounded energy (straight line). Mode 2 matches quite well and mode 3 is essentially a perfect comparison.

One brief side note is in order. Notice that even with the fictitious moon, the perturbations for the inclination mode and the system energy (y_4) are growing with time. The most likely reason for this is that a value larger than one year may be needed for t_1 (§ 5.1).

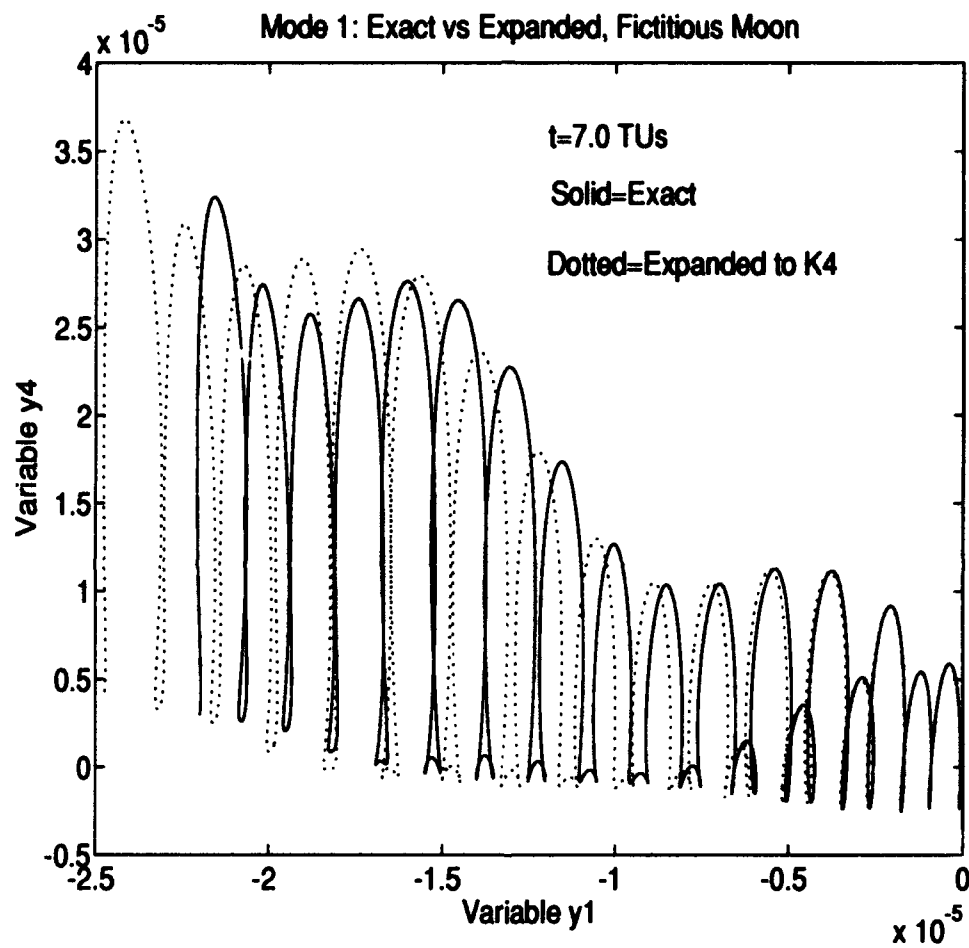


Figure 34. Exact vs Expanded Modal Solution (K2, K3 & K4) for Fictitious Moon. Time/Energy Mode.

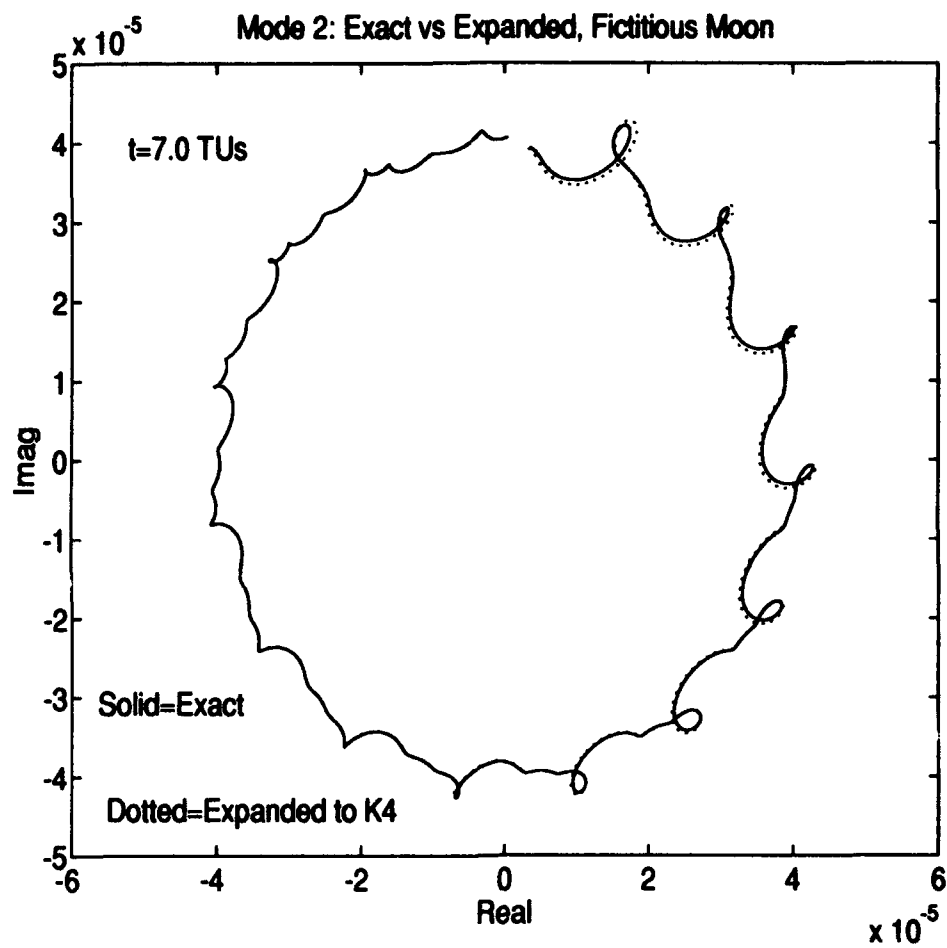


Figure 35. Exact vs Expanded Modal Solution (K2, K3 & K4) for Fictitious Moon. Inclination Mode.

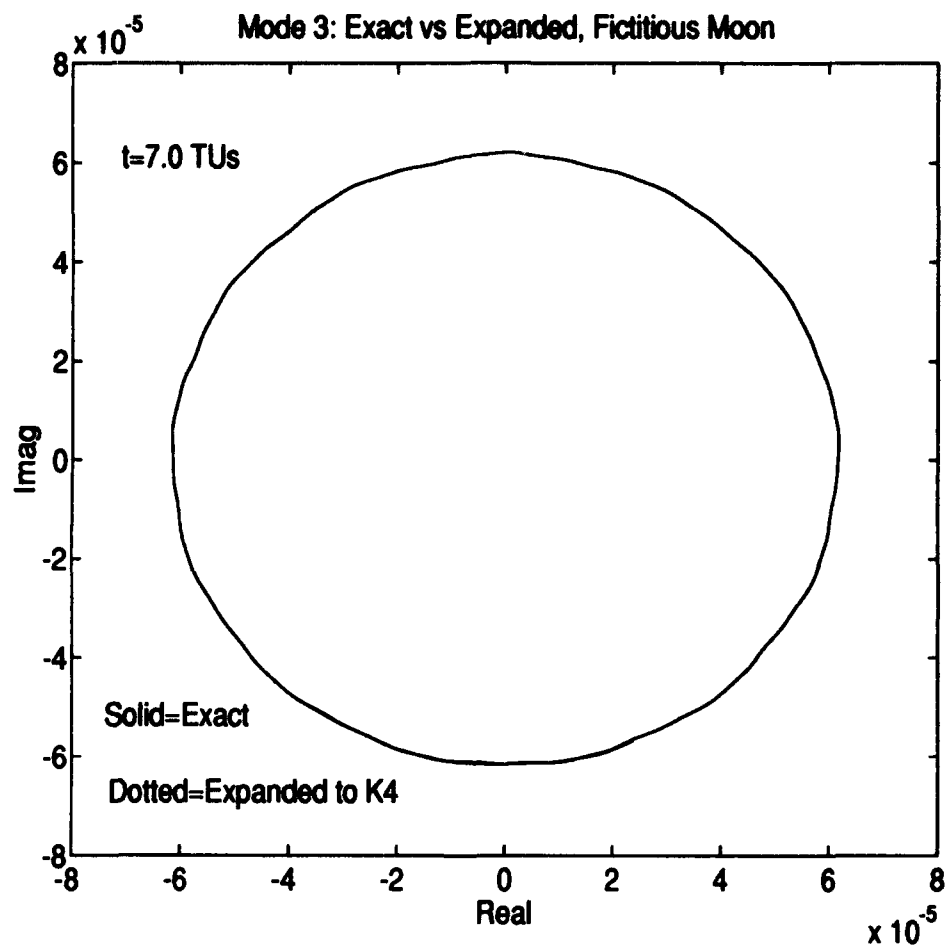


Figure 36. Exact vs Expanded Modal Solution (K2, K3 & K4) for Fictitious Moon. Eccentricity Mode.

Since the new modal plots matched so well, we have shown that the canonical Floquet perturbation theory technique was successfully applied to the moon's orbit and that Eq (92) is a modal solution to the real moon, however a great number of terms would be required in the expansion.

5.3 Complex Conjugacy

In the paper by Wiesel and Pohlen (1992:9), it was assumed that the eigenvector matrix of a Hamiltonian system must always contain complex conjugate eigenvectors to perform a canonical transformation. As it turns out, the eigenvectors of the moon's monodromy matrix does *not* contain complex conjugate eigenvectors. It is concluded, therefore, that symplectic normalization does not necessarily need to involve maintaining complex conjugacy of the eigenvector's from F to E .

VI. Conclusions and Recommendations

The main conclusion of this work is that the canonical Floquet theory technique was successfully applied to the moon's orbit. This study showed that canonical Floquet perturbation theory is applicable to a system which, besides being dynamically more interesting than previous applications, is also constrained to obey real historical data. We used the restricted three body problem to get Hill's lunar orbit as a stable periodic reference orbit, and applied canonical Floquet theory using interpolated initial conditions from real moon ephemerides of February 1967. The moon's interpolated initial position proved to be accurate, but the interpolated initial momenta had to be modified to accommodate the differences in our restricted three body model and the real world dynamics. We successfully fit the initial momenta such that the moon's position, when integrated forward for one year, still matched the data.

The modal plots of the real moon's orbit showed that it was outside the linear region of Hill's periodic orbit, but still close enough to demonstrate the technique. The time/energy mode oscillated, but the energy remained bounded, while the inclination and eccentricity modes oscillated with higher frequency perturbations about an expected perfect circle. We derived the modal solution using both an exact and an expanded modal representation. The Hamiltonian was successfully transformed to modal variables and the modal equations of motion were found out to three expansion terms. We truncated the expanded solution after each of the first three terms and compared the modal plots. The results demonstrated that the exact and expanded representations will agree given that enough expansion terms are included. For the fictitious moon, three terms were sufficient to consider the modal EOM a viable modal solution, however the real moon, being further away from the linear region, requires many more expansion terms.

In future studies, the modal solution found here can be used as the reference trajectory for further analytic perturbation applications such as Von Ziepel's method. In addition, the

higher order expansion terms could be included to completely validate our contention. Also, the fitting of initial momenta to future ephemerides could be extended beyond one year. It might decrease the magnitude of the higher frequency perturbations.

Appendix A: Monodromy Matrix, Initial Eigenvector Matrix, and J Matrix

The following matrices, used for Floquet theory, help describe our periodic orbit and were output from the program PERIOD.

The monodromy matrix $\Phi(\tau, 0)$:

row	column	
1	1	1.095712688474569
2	1	-20.370277922605400
3	1	0.000000000000000E+000
4	1	274.031141304028700
5	1	-1.269564310370324
6	1	0.000000000000000E+000
1	2	6.294761110516258E-001
2	2	8.048342665042469E-001
3	2	0.000000000000000E+000
4	2	1.269564305657530
5	2	-8.349576338746477
6	2	0.000000000000000E+000
1	3	0.000000000000000E+000
2	3	0.000000000000000E+000
3	3	8.601930291457586E-001
4	3	0.000000000000000E+000
5	3	0.000000000000000E+000
6	3	-7.345815692997451
1	4	4.745632093038844E-002
2	4	-1.471358089142643E-002
3	4	0.000000000000000E+000
4	4	1.095712688719114
5	4	-6.294761110578383E-001
6	4	0.000000000000000E+000
1	5	1.471358087321641E-002
2	5	-1.491295028851029
3	5	0.000000000000000E+000
4	5	20.370277922636880
5	5	8.048342661624743E-001
6	5	0.000000000000000E+000

monodromy matrix (cont.)

row	column	
1	6	0.000000000000000E+000
2	6	0.000000000000000E+000
3	6	3.540354992250493E-002
4	6	0.000000000000000E+000
5	6	0.000000000000000E+000
6	6	8.601930291462128E-001

The initial eigenvector matrix $F(0)$:

row	column	(real , imaginary)
1	1	(-8.192793633048179E-014,2.007180267772390E-027)
2	1	(-7.539018574763626E-002,1.667302866291538E-017)
3	1	(-1.217710722943405E-019,4.972171594093748E-023)
4	1	(1.000000000000000,0.000000000000000E+000)
5	1	(-1.361796347709330E-011,-1.305682296333588E-026)
6	1	(-9.189976165277692E-019,2.610493483499758E-023)
1	2	(-7.539018574755219E-002,-1.439135915971290E-012)
2	2	(1.405590215265010E-011,-1.021808214943804E-001)
3	2	(-3.808102176268219E-017,2.617711356936501E-018)
4	2	(-1.757523295343237E-010,6.646921145391658E-001)
5	2	(1.000000000000000,0.000000000000000E+000)
6	2	(-1.999332831133622E-017,-4.141361260090141E-017)
1	3	(8.609626586666082E-017,-1.470913273776291E-017)
2	3	(-9.403731537416513E-017,-4.199563329593159E-016)
3	3	(3.092693812092022E-014,-6.942300233683507E-002)
4	3	(1.391287225318998E-015,6.660459595692267E-015)
5	3	(-1.332598592779162E-015,3.703060854033629E-016)
6	3	(1.000000000000000,0.000000000000000E+000)
1	4	(3.589486770491939E-003,0.000000000000000E+000)
2	4	(0.000000000000000E+000,0.000000000000000E+000)
3	4	(0.000000000000000E+000,0.000000000000000E+000)
4	4	(0.000000000000000E+000,0.000000000000000E+000)
5	4	(-2.334981756025643E-002,0.000000000000000E+000)
6	4	(0.000000000000000E+000,0.000000000000000E+000)

initial eigenvector matrix (cont.)

row	column	(real , imaginary)
1	5	(-7.539018574755219E-002,1.439135915971290E-012)
2	5	(1.405590215265010E-011,1.021808214943804E-001)
3	5	(-3.808102176268219E-017,-2.617711356936501E-018)
4	5	(-1.757523295343237E-010,-6.646921145391658E-001)
5	5	(1.000000000000000,0.000000000000000E+000)
6	5	(-1.999332831133622E-017,4.141361260090141E-017)
1	6	(8.609626586666082E-017,1.470913273776291E-017)
2	6	(-9.403731537416513E-017,4.199563329593159E-016)
3	6	(3.092693812092022E-014,6.942300233683507E-002)
4	6	(1.391287225318998E-015,-6.660459595692267E-015)
5	6	(-1.332598592779162E-015,-3.703060854033629E-016)
6	6	(1.000000000000000,0.000000000000000E+000)

The J matrix:

row	column	(real , imaginary)
1	1	(0.000000000000000E+000,0.000000000000000E+000)
2	1	(0.000000000000000E+000,0.000000000000000E+000)
3	1	(0.000000000000000E+000,0.000000000000000E+000)
4	1	(0.000000000000000E+000,0.000000000000000E+000)
5	1	(0.000000000000000E+000,0.000000000000000E+000)
6	1	(0.000000000000000E+000,0.000000000000000E+000)
1	2	(0.000000000000000E+000,0.000000000000000E+000)
2	2	(0.000000000000000E+000,8.853941825307000E-001)
3	2	(0.000000000000000E+000,0.000000000000000E+000)
4	2	(0.000000000000000E+000,0.000000000000000E+000)
5	2	(0.000000000000000E+000,0.000000000000000E+000)
6	2	(0.000000000000000E+000,0.000000000000000E+000)
1	3	(0.000000000000000E+000,0.000000000000000E+000)
2	3	(0.000000000000000E+000,0.000000000000000E+000)
3	3	(0.000000000000000E+000,1.053464567610000)
4	3	(0.000000000000000E+000,0.000000000000000E+000)
5	3	(0.000000000000000E+000,0.000000000000000E+000)
6	3	(0.000000000000000E+000,0.000000000000000E+000)

J matrix (cont.)

row	column	(real , imaginary)
1	4	(1.000000000000000,0.000000000000000E+000)
2	4	(0.000000000000000E+000,0.000000000000000E+000)
3	4	(0.000000000000000E+000,0.000000000000000E+000)
4	4	(0.000000000000000E+000,0.000000000000000E+000)
5	4	(0.000000000000000E+000,0.000000000000000E+000)
6	4	(0.000000000000000E+000,0.000000000000000E+000)
1	5	(0.000000000000000E+000,0.000000000000000E+000)
2	5	(0.000000000000000E+000,0.000000000000000E+000)
3	5	(0.000000000000000E+000,0.000000000000000E+000)
4	5	(0.000000000000000E+000,0.000000000000000E+000)
5	5	(0.000000000000000E+000,-8.853941825307000E-001)
6	5	(0.000000000000000E+000,0.000000000000000E+000)
1	6	(0.000000000000000E+000,0.000000000000000E+000)
2	6	(0.000000000000000E+000,0.000000000000000E+000)
3	6	(0.000000000000000E+000,0.000000000000000E+000)
4	6	(0.000000000000000E+000,0.000000000000000E+000)
5	6	(0.000000000000000E+000,0.000000000000000E+000)
6	6	(0.000000000000000E+000,-1.053464567610000)

Appendix B: Ephemerides from February 1967

The following data was collected from the *American Ephemeris and Nautical Almanac* (U.S. Naval Observatory, 1967:19,53) for February 1967:

Date/Time	Moon's Apparent Longitude			Moon's Apparent Latitude		
	°	'	"	°	'	"
7 Feb / 0000 UT	289.d0	15.d0	55.35d0	-4.d0	38.d0	35.46d0
8 Feb / 0000 UT	301.d0	56.d0	55.63d0	-4.d0	56.d0	09.13d0
9 Feb / 0000 UT	314.d0	27.d0	13.68d0	-4.d0	59.d0	07.25d0
10 Feb / 0000 UT	326.d0	46.d0	52.49d0	-4.d0	47.d0	57.13d0
11 Feb / 0000 UT	338.d0	56.d0	15.14d0	-4.d0	23.d0	42.42d0

Date/Time	Moon's Horizontal Parallax			Sun's Longitude		
	°	'	"	°	'	"
7 Feb / 0000 UT	0.d0	56.d0	01.692d0	317.d0	31.d0	10.3d0
8 Feb / 0000 UT	0.d0	55.d0	34.266d0	318.d0	31.d0	58.3d0
9 Feb / 0000 UT	0.d0	55.d0	09.022d0	319.d0	32.d0	45.2d0
10 Feb / 0000 UT	0.d0	54.d0	46.509d0	320.d0	33.d0	30.8d0
11 Feb / 0000 UT	0.d0	54.d0	27.580d0	321.d0	34.d0	15.0d0

Appendix C: Ephemerides from February 1986

This appendix contains the information that was used to run the alternate new moon data for verification of the errors in the preliminary results. The following data was collected from *The Astronomical Almanac* (U.S. Naval Observatory, 1986:C4,D6) for February 1986:

Date/Time	Moon's Apparent Longitude °	Moon's Apparent Latitude °
7 Feb / 0000 UT	291.38d0	-4.91d0
8 Feb / 0000 UT	305.52d0	-5.01d0
9 Feb / 0000 UT	319.44d0	-4.81d0
10 Feb / 0000 UT	333.07d0	-4.34d0
11 Feb / 0000 UT	346.35d0	-3.64d0

Date/Time	Moon's Horizontal Parallax ° ' "			Sun's Longitude ° ' "		
7 Feb / 0000 UT	0.d0	59.d0	05.18d0	317.d0	55.d0	01.47d0
8 Feb / 0000 UT	0.d0	58.d0	41.18d0	318.d0	55.d0	49.69d0
9 Feb / 0000 UT	0.d0	58.d0	09.23d0	319.d0	56.d0	36.72d0
10 Feb / 0000 UT	0.d0	57.d0	31.30d0	320.d0	57.d0	22.47d0
11 Feb / 0000 UT	0.d0	56.d0	50.16d0	321.d0	58.d0	06.84d0

The new moon selected from 1986 occurred on 9 February 1986 at 0055 UT, therefore the interpolation variables and subsequent initial state vector for this case are:

$$h = 1.0 \text{ (days)} \quad a = \frac{55.0}{1440.0} \text{ (days)}$$

$$u_{-2} = 7 \text{ Feb } 0000 \text{ UT}$$

$$u_{-1} = 8 \text{ Feb } 0000 \text{ UT}$$

$$u_0 = 9 \text{ Feb } 0000 \text{ UT}$$

$$u_1 = 10 \text{ Feb } 0000 \text{ UT}$$

$$u_2 = 11 \text{ Feb } 0000 \text{ UT}$$

$$\bar{x}(0) = [-0.99748 \quad -6.9847E-7 \quad -2.1084E-4 \quad 1.5751E-3 \quad -0.96495 \quad 7.7049E-4]^T$$

Bibliography

- Abramowitz, Milton and Irene A. Stegun. *Handbook of Mathematical Functions*. New York: Dover Publications, Inc., 1965.
- Bate, Roger R., Donald D. Mueller, and Jerry E. White. *Fundamentals of Astrodynamics*. New York: Dover Publications, Inc., 1971.
- Brouwer, Dirk and Gerald M. Clemence. *Methods of Celestial Mechanics*. New York and London: Academic Press, 1961.
- Brown, Ernest W. *An Introductory Treatise on the Lunar Theory*. New York: Dover Publications, Inc., 1960.
- Meirovitch, Leonard. *Methods of Analytical Dynamics*. New York: McGraw-Hill Book Company, 1970.
- Pars, L.A. *A Treatise on Analytical Dynamics*. New York: John Wiley and Sons, 1965.
- Pohlen, Capt David J. *Canonical Floquet Perturbation Theory*. MS thesis, AFIT/GA/ENY/92D-03. School of Engineering, Air Force Institute of Technology (AU), Wright-Patterson AFB OH, December 1992.
- Ross, Capt David A. *Perturbation Theory for Restricted Three-Body Orbits*. MS thesis, AFIT/GA/ENY/91D-07. School of Engineering, Air Force Institute of Technology (AU), Wright-Patterson AFB OH, December 1991.
- Siegel, Carl L. and Jürgen K. Moser. *Lectures on Celestial Mechanics*. Translation by C.I. Kalme. Berlin, Heidelberg, and New York: Springer-Verlag, 1971.
- Szebehely, Victor. *Theory of Orbits*. New York and London: Academic Press, 1967.
- United States Naval Observatory. *The American Ephemeris and Nautical Almanac for the Year 1967*. Washington, D.C.: U.S. Government Printing Office, 1967.
- United States Naval Observatory. *The Astronomical Almanac, 1986*. Washington, D.C.: U.S. Government Printing Office, 1986.
- Wiesel, William E. "Perturbation Theory in the Vicinity of a Periodic Orbit by Repeated Linear Transformations," *Journal of Celestial Mechanics*, 23: 231-242 (1980).
- Wiesel, William E. "Floquet Reference Solutions for the Lunar Theory and the Jovian Moons," *Journal of Guidance and Control*, 4: 586-590 (1981).
- Wiesel, William E. *Spaceflight Dynamics*. New York: McGraw-Hill Book Company, 1989.

Wiesel, William E. and David J. Pohlen. "Canonical Floquet Theory." Article for Journal Submission (October 1992).

Wiesel, William E., Professor of Astronautics, *Course text distributed in Mech 636, Advanced Astrodynamics*. School of Engineering, Air Force Institute of Technology (AU), Wright-Patterson AFB OH, January 1993.

Vita

Capt Kurt A Vogel was born on 16 February 1967 in Anchorage, Alaska. Upon graduation from Clayton Valley High School in Concord, California in 1985, he received a presidential nomination to the U.S. Air Force Academy. In 1989, he graduated with a Bachelor of Science in Astronautical Engineering and received a regular commission in the USAF. On 10 June 1989, he married Tracy Michele Farrar at the Presidio in San Francisco, California. His first assignment was to Kirtland AFB in Albuquerque, New Mexico. As a Spacecraft Systems Analyst in the Weapons Laboratory Space Experiments Office, he designed, built, tested, and integrated in-house experiments to be flown in space. In 1990, he was selected for transfer into the Phillips Laboratory Optical Surveillance Division, where he provided critical orbital analyses to a presidentially directed, highly classified program. In 1992, he attended the Air Force Institute of Technology, School of Engineering. Following graduation from AFIT with a Master of Science in Astronautical Engineering, he was assigned to the Consolidated Space Test Center at Onizuka AFB in Sunnyvale, California.

Permanent Address: 5210 Jomar Drive
Concord, California 94521

REPORT DOCUMENTATION PAGE			Form Approved OMB No. 0704-0188	
<small>Public reporting burden for this collection of information is estimated to average 1 hour per response, including the time for reviewing instructions, searching existing data sources, gathering and maintaining the data needed, and completing and reviewing the collection of information. Send comments regarding this burden estimate or any other aspect of this collection of information, including suggestions for reducing this burden, to Washington Headquarters Services, Directorate for Information Operations and Reports, 1215 Jefferson Davis Highway, Suite 1204, Arlington, VA 22202-4302, and to the Office of Management and Budget, Paperwork Reduction Project (0704-0188), Washington, DC 20503.</small>				
1. AGENCY USE ONLY (Leave blank)		2. REPORT DATE December 1993		3. REPORT TYPE AND DATES COVERED Master's Thesis
4. TITLE AND SUBTITLE THE MODAL SOLUTION TO THE MOON'S ORBIT USING CANONICAL FLOQUET PERTURBATION THEORY			5. FUNDING NUMBERS	
6. AUTHOR(S) Kurt A. Vogel, Captain, USAF				
7. PERFORMING ORGANIZATION NAME(S) AND ADDRESS(ES) Air Force Institute of Technology, WPAFB, OH 45433-6583			8. PERFORMING ORGANIZATION REPORT NUMBER AFTT/GA/ENY/93D-9	
9. SPONSORING / MONITORING AGENCY NAME(S) AND ADDRESS(ES) Phillips Laboratory PL/VTA, Kirtland AFB, NM 87117-6008			10. SPONSORING / MONITORING AGENCY REPORT NUMBER	
11. SUPPLEMENTARY NOTES				
12a. DISTRIBUTION / AVAILABILITY STATEMENT Approved for public release; distribution unlimited			12b. DISTRIBUTION CODE	
13. ABSTRACT (Maximum 200 words) Using the restricted three body problem, the equations of motion (EOM) and Hamiltonian are computed for the moon's orbit in physical variables. A periodic orbit is found in the vicinity of the moon's orbit, and classical Floquet theory is applied to the periodic orbit to give stability information and the complete solution to the equations of variation. Floquet theory also supplies a transformation from physical variables to modal variables. This transformation to modal variables is made canonical by constraining the initial transformation matrix to be symplectic. Actual lunar data is used to calculate the modes for the real moon's orbit. Once satisfied that the moon's real-world modes are in (or near) the linear regime of the periodic orbit, the modal EOM are found by doing a perturbation expansion on the new modal Hamiltonian. The modal results from the real lunar orbit are compared with the modal EOM/expansion results. The modal expansion proves to be an accurate solution to the moon's orbit given enough expansion terms.				
14. SUBJECT TERMS Lunar Theory, Moon's Orbit, Modal Variables, Modal Reference Solutions Floquet Theory, Canonical Systems, Perturbation Theory, Periodic Orbits			15. NUMBER OF PAGES 98	
			16. PRICE CODE	
17. SECURITY CLASSIFICATION OF REPORT Unclassified	18. SECURITY CLASSIFICATION OF THIS PAGE Unclassified	19. SECURITY CLASSIFICATION OF ABSTRACT Unclassified	20. LIMITATION OF ABSTRACT UL	